

Analysis of Linear and Non-Linear Stress-Strain Properties for Graphene and Single Walled Carbon Nanotubes

Submitted by
Sathish Kumar Garala
(ME10M11)

Under the Guidance of
Dr. Ashok Kumar Pandey
Assistant Professor
Department of Mechanical Engineering

A Dissertation Submitted to
Indian Institute of Technology Hyderabad
in Partial Fulfillment of the Requirements for
The Degree of Master of Technology



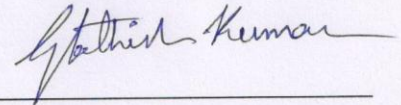
भारतीय प्रौद्योगिकी संस्थान हैदराबाद
Indian Institute of Technology Hyderabad

Department of Mechanical Engineering
Indian Institute of Technology, Hyderabad – 502205.

July, 2012

Declaration

I declare that this written submission represents my ideas in my own words, and where others' ideas or words have been included, I have adequately cited and referenced the original sources. I also declare that I have adhered to all principles of academic honesty and integrity and have not misrepresented or fabricated or falsified any idea/data/fact/source in my submission. I understand that any violation of the above will be a cause for disciplinary action by the Institute and can also evoke penal action from the sources that have thus not been properly cited, or from whom proper permission has not been taken when needed.



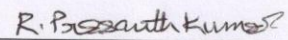
(Signature)

Sathish Kumar Garala

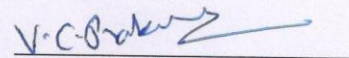
ME10M11

Approval Sheet

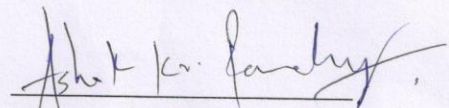
This thesis entitled **Analysis of Linear and Non-Linear Stress-Strain Properties for Graphene and Single Walled Carbon Nanotubes** by Sathish Kumar Garala is approved for the degree of Master of Technology from IIT Hyderabad.



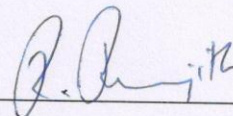
Dr. R. Prasanth Kumar
Assistant Professor
Department of Mechanical Engineering
Examiner



Dr. Chandrika Prakash Vyasrayani
Assistant Professor
Department of Mechanical Engineering
Examiner



Dr. Ashok Kumar Pandey
Assistant Professor
Department of Mechanical Engineering
Adviser



Dr. Ranjith Ramadurai
Assistant Professor
Department of Materials Science & Engineering
Chairman

Acknowledgements

It is a great experience and learning for having worked with one of the country's premier institute of technology, IIT Hyderabad. It's a memorable journey for me to evaluate myself professionally which helped in overall self-development. For now, it gives me an immense pleasure to thank the great minds behind my successful completion of M. Tech Thesis work. It gives me pleasure in thanking **Prof. U. B Desai**, Director, IIT Hyderabad for providing us with the necessary infrastructure and the professional support at all times

I am so grateful to my thesis guide **Dr. Ashok Kumar Pandey**, Assistant Professor, Department of Mechanical Engineering, for providing excellent guidance, consistent encouragement, inspiration and motivation to stay focused throughout the research work. Without his invaluable guidance, this work would never have been a successful one.

I also wish to thank **Prof. Vinayak Eswaran**, H.O.D, Department of Mechanical Engineering, for his kind cooperation and support extended through the department as and when required.

I want to thank **Dr. G. Prabusankar**, Assistant Professor, Department of Chemistry, **Mr. Guru Prasath Ravindran** (Project Associate) and research scholar **Md. Kushafudoja**, Department of Mechanical Engineering for the fruitful discussions.

I would like to extend my gratitude to all the faculty members for their care and support which helped us grow our attitude and character along with the professional skills.

I would like to thank Staff members of the Institute, Project Associate Staff of CAE Lab, Research scholars and M Tech colleagues of Department of Mechanical Engineering for their help and support, whenever needed.

I am also thankful to all my friends at IIT Hyderabad, especially M. Tech Design Engineering students, for providing a stimulating and fun environment and making my stay in the institute campus a pleasure and also helping me in all the ways professionally and personally.

Lastly, and most importantly, I want to thank my parents, **Smt. S. Reddemma** and **Sri. G. Rajagopal**, for their blessings, love and support.

Dedicated to

My Parents, Sri **S. Reddemma** & Sri **G. Raja Gopal**

My brother **G. V. V. S. Reddy Prasad**

My beloved Grand Father Late Sri **G. H. Krishna Moorthy**

&

With all due respect and faith

Lord Sri Venkateswara Swamy

Abstract

Carbon Nanotube (CNT) has revolutionized the world of nanotechnology with several novel applications in the field of sensors and actuators. Such popularity of CNT is due to its excellent mechanical and electrical properties. There are several studies done on understanding the modeling of mechanical and electrical properties using different approaches ranging from molecular to continuum based method. In this thesis, we focus on estimating the mechanical properties of single walled carbon nanotube (SWCNT) mainly based on stress-strain relationship.

There are several approaches such as molecular mechanics, molecular dynamics, coupled molecular-structural mechanics, exponential Cauchy born based continuum method, etc, for estimating the linear and nonlinear stress-strain relationship in order to find elastic modulus of SWCNT. In this thesis, we first find the analytical model using molecular mechanics approach to study the variation of elasticity with the diameter of SWNT under different configurations. It is found that the elasticity becomes size independent if the diameter is above 1 nm. Moreover this approach does not help us to get accurate nonlinear stress-strain relationship. Therefore, we used coupled molecular-structural approach to study the nonlinear variation of stress-strain relationship for different configurations. Then, we come up with compact formulas in order to predict the nonlinear stress-strain relationship. Capitalizing on this approach, we find the equivalent mechanical properties of a beam element for the corresponding C-C bond that exists in CNT. Thereafter, we use these properties to do structural modeling in ANSYS which drastically reduces the modeling effort as compared to molecular dynamics approach. In order to standardize this approach, we do several comparisons and tests with existing results based on other methods. It is found that the results are in good agreement with the literature. After validating the stress-strain properties of SWCNT under different configurations, we do modal analysis to find the first few frequencies for fixed-fixed and cantilever kinds of support. On comparing the results with analytical model based from continuum theory, we get relatively good match for cantilever under

wider range of aspect ratio- a ratio of length to diameter of SWNT. However, analytical result for the fixed-fixed condition matches well only for larger length to diameter ratio. Furthermore, we investigate different modes of graphene and SWCNT under different configurations to demonstrate the capabilities of this method.

Finally, we develop an approach based on coupled molecular-structural mechanics method keeping in mind two main objectives. First, to reduce the simulation time and second is to generate different configuration of SWNT. The method developed in this thesis can be utilized to study different aspect of multi-walled carbon nanotubes. However, applicability of the method can be increased by validating the approach with more experimental results.

Nomenclature

CNT – Carbon Nanotube

SWCNT – Single Walled Carbon Nanotube

MWCNT – Multi Walled Carbon Nanotube

CVD – Chemical Vapor Decomposition

C – Chiral vector

Φ - Chiral angle

T - Translation vector

$H_I(r_{ij})$ – Interatomic and intermolecular potential

r_{ij} – Bond Distance between atoms i and j

H_{rep} - Repulsive interaction energy

H_{att} - Attractive interaction energy

E_b – Chemical binding energy

MD – Molecular Dynamics

STM - Scanning Tunneling Microscope

AFM - Atomic force microscope

SFM - scanning force microscope

TEM - Transmission Electron Microscope

U – Total potential energy

$U_{stretch}$, U_r – Potential energy corresponding to stretching

$U_{bending}$, U_θ – Potential energy corresponding to stretching

$U_{torsion}$, U_T – Potential energy corresponding to torsion

U_{vdW} – Potential energy corresponding to Van der Waals forces

Y_s - Young's Modulus

K_ρ - Axial spring stiffness

K_θ - Spiral spring stiffness

β_1, D_e, K_θ are Morse-Modified Potential constants

t - Thickness of the CNT

FEM – Finite Element Method

U_A – strain energy under pure tension

U_M – strain energy due to bending

U_T – strain energy due to torsion

E - Elasticity of Beam

I – Moment of Inertia

G - Rigidity Modulus

d – diameter of beam element

k_r, k_θ, k_T - Force Constants

L/D – Length to diameter ratio of CNT

f_n – Fundamental frequency

Contents

Acknowledgements.....	iv
Abstract.....	vi
Nomenclature	viii
1 Introduction.....	1
1.1 Carbon Nanotubes	1
1.1.1 Application of CNTs	1
1.1.2 Characterization of CNTs.....	1
1.2 Important parameters of CNTs	2
1.2.1 Geometry and Configuration of CNTs	2
1.2.2 Classification of CNTs	3
1.3 Inter-atomic potentials used in CNTs	4
1.4 Literature Survey on analysis of mechanical properties of CNTs	6
2 Analytical Studies on Carbon Nanotubes.....	7
2.1 Various approaches available for studies on CNTs	7
2.2 Experimental Approach	7
2.3 Molecular Mechanics Approach.....	8
2.3.1 CNT size effects on Elasticity	9
2.3.2 Stress-Strain Relationship for Armchair CNT	12
2.3.3 Stress-Strain Relationship for zigzag CNT	16
3 Numerical analysis of Carbon Nanotube.....	19
3.1 Beam Element Modeling of CNT	19
3.2 Modeling tools and approach for ANSYS analysis	20
3.3 Scaling Factors and details of CNT/Graphene Models on ANSYS.....	22
3.4 Comparison of the ANSYS simulation results	23
4 Modal Analysis of CNTs	27
4.1 Continuum Models for Modal Analysis	27
4.2 Bending Modes and Fundamental Frequencies	29
4.3 Different modes of vibrations	31
5 Conclusion	37
5.1 Conclusion	37
References.....	38

Chapter 1

Introduction

1.1 Carbon Nanotubes

The carbon nanotubes (CNTs), since their discovery in the year 1991 by Iijima, have evolved to be an interesting field of research. These nanotubes fall in the fullerenes structural family which is sometimes capped by bucky ball structure. The diameter of the carbon nanotubes will be in the range of nanometers, while the length can go upto 18 centimeters, and hence length to diameter ratio is extremely high. The methods of synthesizing the CNTs essentially require the pyrolysis or the thermal decomposition of an appropriate carbon source, such as hydrocarbons or carbon monoxide. The three popular techniques for synthesizing CNTs are the chemical vapor decomposition (CVD), arc discharge and Laser Ablation. These methods produce variety of nanotubes with a distribution of diameter. [1-3]

1.1.1 Application of CNTs

The CNTs have a huge range of applications in the field of nanotechnology, because of their excellent mechanical and electrical fields. The structural applications include the composites; light weight sports goods, bullet proof jackets and many others. CNTs can act as very good super conductors at low temperatures, field emitting transistors and have varied electromagnetic applications. They are even used for the physical and chemical sensing devices such as the electrochemical sensors, resonator sensors, thermal sensors, optical sensors, flow sensors, force sensors, electromechanical actuators, acoustic sensors etc. Even in the field of medicine, these are exclusively used as Bio-sensors.

1.1.2 Characterization of CNTs

The usage of the CNTs in such a wide range of applications can be done only when there are studies to have a basic level characterization of its properties. The characterization involves the study of the physical, electrical, magnetic, chemical and mechanical properties of the CNTs. The mechanical characterization of the CNTs deals with the measurement and analysis of the hardness, elastic modulus, viscoelastic properties, and localized deformation studies. These studies at the atomic and molecular sizes, needs a state-of-art theories and

experiments to be conducted for the evaluation to be perfect. In this study an emphasis is made on predicting the elasticity of the CNTs using the existing theories. The elasticity of CNTs is most essential in establishing the mathematical modeling of mechanical applications at nano-scale.

1.2 Important parameters of CNTs

1.2.1 Geometry and Configuration of CNTs

The atomic structure of nanotubes can be described in terms of the tube chirality, or helicity, which is defined by the chiral vector C the chiral angle Φ (figure 1). The graphene sheet is cut along the dotted lines as shown in figure and the then rolled such that the tip of the chiral vector touches its tail. The chiral vector is also known as the roll up vector and is given as

$$C = na + mb \quad (1)$$

Where a, b are the unit base vectors and n, m are the integers.

Based on the chiral vector and the chiral angle, three configurations of nanotubes are available (figure 1&2).

- The zig-zag configuration has a chiral angle of 0 degrees represented by a chiral vector $(n,0)$
- The arm-chair configuration has a chiral angle of 30 degrees represented by a chiral vector (n,n)
- The chiral configuration has a chiral angle of $0 < \Phi < 30$ degrees represented by a chiral vector (n,m)

Another important geometrical parameter is the translation vector T , which is perpendicular to the chiral vector C and is given as

$$T = \frac{2m+n}{d}a - \frac{2n+m}{d}b \quad (2)$$

Where $d = \text{gcd}(2n + m, 2m + n)$

The diameter of the CNT is given in terms of the C-C bond length r_0 and the chiral indices n, m as below,

$$\text{Diameter of the CNT} = D_{\text{CNT}} = \frac{3r_0}{\pi} \sqrt{n^2 + m^2 + mn}$$

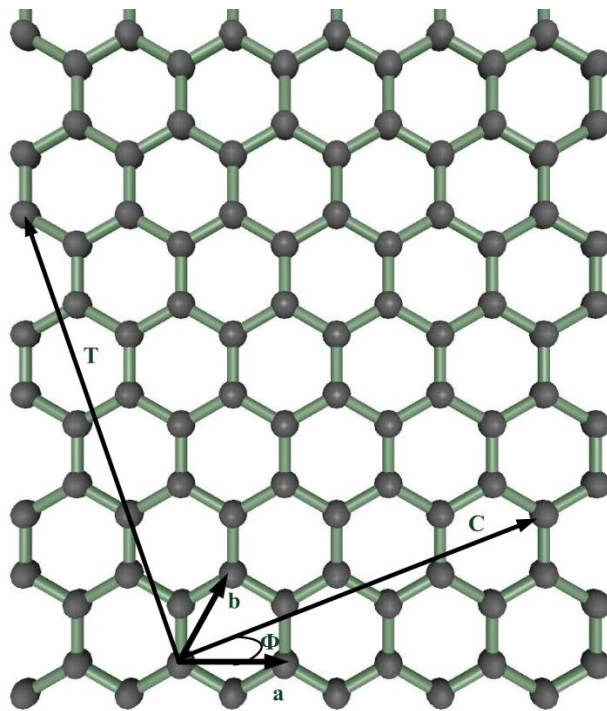


Fig 1: Graphene sheet with the unit vectors, chiral vector, the translation vector

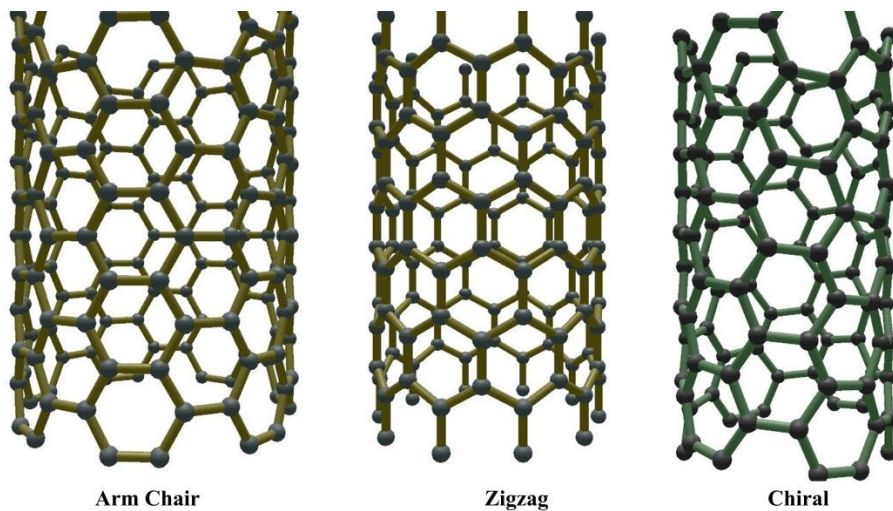


Fig 2: CNT configurations Arm-chair, zig-zag and chiral

1.2.2 Classification of CNTs

The CNTs are broadly classified into Single Walled Nanotubes (SWNT) and Multi Walled Nanotubes (MWNT). The SWNT can be visualized as wrapping of one atom layer thick graphene sheet into a seamless cylinder. Single-walled nanotubes are an important variety of carbon nanotube because they exhibit electric properties that are not shared by the multi-walled carbon nanotube (MWNT) variants.[1-3]

Multi-walled nanotubes (MWNT) consist of multiple rolled layers (concentric tubes) of graphite. There are two models describing the structures of multi-walled nanotubes. (a) Russian Doll model - sheets of graphite are arranged in concentric cylinders, e.g. a (0,8) single-walled nanotube (SWNT) within a larger (0,17) single-walled nanotube; (b) Parchment model - a single sheet of graphite is rolled in around itself, like a scroll of parchment or a rolled newspaper. The interlayer distance in multi-walled nanotubes is approximately 3.4 Å.

1.3 Inter-atomic potentials used in CNTs

A branch of nanotechnology, Computational nanotechnology deals with the mathematical modeling and the computer based simulations to predict and compute the dynamics of nanostructures. This area widely employs the concepts from the classical and quantum mechanical many-body theories on which a study of the formation, evolution and the properties of nanostructures and the mechanisms of Nano process. This can be achieved by performing atom-by-atom modeling and simulations. The precision of this numerical analysis depends on the accuracy of the interatomic and intermolecular potentials energy functions used. These potentials are heavily used in the computational analysis of the nanostructures. The most widely used approaches used in modeling of these nanostructures composed of several millions of atoms, using the above potentials, are Monte Carlo Simulation and the molecular dynamics simulation.

The forces experienced by the atoms and molecules are obtained from prescribed two-body or many-body interatomic and intermolecular potentials, $H_I(r_{ij})$, according to

$$F_i = - \sum_{j>1} \nabla_i H_I(r_{ij}) \quad (3)$$

Where r_{ij} is the separation distance between two particles i and j

Intermolecular potential energies include pairwise additive energies as well as many-body interactions. The inter-particle interaction potential energy between molecules or atoms is represented as

$$H(r) = H_{\text{rep}} + H_{\text{att}} \quad (4)$$

Where r is the intermolecular distance, H_{rep} and H_{att} are the repulsive and the attractive interaction energies respectively.

The interaction force (F) is thus given as

$$F = -\nabla H(r) \quad (5)$$

The important pairwise additive energies include the repulsive potentials, van der Waals energies, interactions involving polar and polarization of molecules, interactions involving the hydrogen bonding and the strong intermolecular energies which include covalent and coulomb interactions. [5-7]

Abell originally derived the general analytic form of the intra-molecular potential energy from the chemical pseudo-potential theory. Abell gave an expression for the chemical binding energy E_b over the nearest neighbours as –

$$E_b = \sum_i \sum_{j(>i)} V^R(r_{ij}) + b_{ij}V^A(r_{ij}) \quad (6)$$

The functions $V^R(r_{ij})$ and $V^A(r_{ij})$ are pair-additive interactions that represent all interatomic repulsions and attraction from valence electrons, respectively. r_{ij} is the distance between pairs of nearest-neighbor atoms i and j , and b_{ij} is a bond order between atoms i and j .

There are many interatomic potential models available for different class of materials. But as we are dealing with the CNTs in our current studies, the C-C covalent bond interatomic potentials that were of importance are Tersoff Many-body Potential Model, Brenner-Tersoff First Generation Hydrocarbon Potentials, Brenner-Tersoff Second-Generation Hydrocarbon Potentials, Modified Morse Potential.

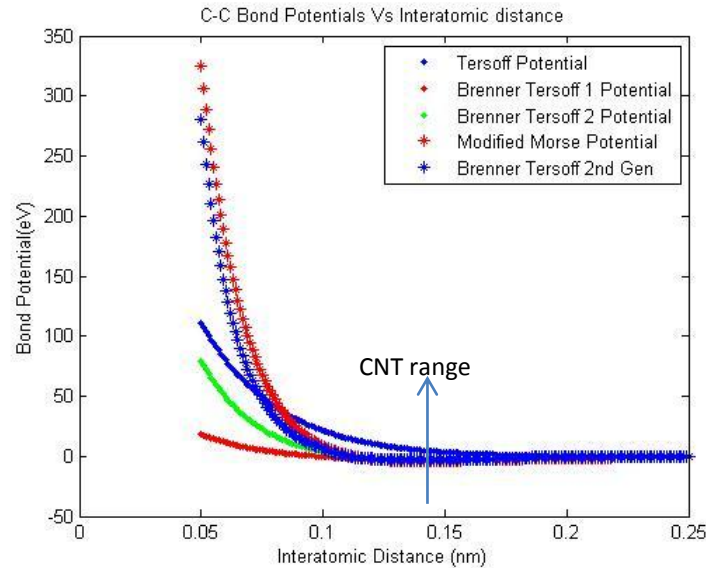


Fig 3: Plot of Bond Potential vs Interatomic Distance for different C-C covalent bond potentials

The non-bonding potentials include the weak van der Waals interactions and others. The Lennard-Jones and Kihara potentials can be used to define the intermolecular interactions between carbon clusters (such as C₆₀) and between the basal planes in a graphite lattice. For a range of interatomic distance ranging from 0.05nm to 2.5nm, the comparison of different potential models as evaluated on MATLAB is represented in Figure (3)

1.4 Literature Survey on analysis of mechanical properties of CNTs

Lourie et al.,[8] using the Raman Spectroscopy, evaluated the Young's modulus of single- and multiwall nanotubes using the D*-band shift method experimentally. Tienchong Chang et al.,[10] predicted the chirality and size dependent elastic properties of SWCNT using stick-spiral model via a molecular mechanics approach. J.R. Xiao et al.,[11] used the stick-spiral model to numerically evaluate the stress-strain relationship for the CNT structures considering a single unit. Tserpes et al.,[14] formulated a linkage parameters between the molecular mechanics and structural mechanics that can be used in the Finite Element Analysis of the CNTs. Ehsan Mohammadpour et al.,[16] used the approach of the Tserpes to model the CNTs in ANSYS. An elaborate detail of the different approaches used in the present study are discussed in the later chapters.

Chapter 2

Analytical Studies on Carbon Nanotubes

2.1 Various approaches available for studies on CNTs

There are experimental, theoretical and numerical studies available to analyze the mechanical properties of Carbon Nanotubes. The experimental procedures on CNTs are very expensive and complicated. The theoretical approach utilizes the principles of the nano-mechanics field in the mechanical characterization of the CNTs. Also the interatomic potentials form the base within the classical multi-body dynamics to provide deterministic mechanical models of CNTs at the atomic scale/resolution. Numerical methods of solution of these models are called molecular dynamics (MD), [13] and sometimes molecular mechanics.

2.2 Experimental Approach

As we are dealing with the sizes at atomic and molecular levels, the apparatus that can handle the test specimen and taking the measurements is a tough job. With the molecular and atomic interactions coming into action, which are normally neglected in macroscopic experiments, should also be given high priority for the final evaluation of the desired properties. Often indirect experimental methods are utilized to overcome such problems. Still the challenges existing even with the most sophisticated experimental apparatus.

The commonly used apparatus in the experimental setup is the scanning tunneling microscope (STM) which is used to image the surfaces at atomic level. Atomic force microscope (AFM) or scanning force microscope (SFM) is the high-resolution type scanning probe microscope. The indirect experimental procedures involve the Micro-Raman spectroscopy which is used to monitor the compressive deformation of the carbon nanotubes embedded in an epoxy matrix. Then using a concentric cylinder model for thermal stresses, the elastic modulus is calculated from the D^* band shift. [8] The elasticity is also estimated by observing the freestanding room temperature vibrations of the SWNT using Transmission Electron Microscope (TEM).[9]

Also many other experimental techniques are available which give a good hope in evaluating the mechanical properties with better accuracy.

2.3 Molecular Mechanics Approach

Molecular Mechanics approach is a statistical mechanics approach, used at a nano-scale, which uses the concepts of the valency and bonding. The molecules are constructed with the balls (atoms) and springs (bonds) where in the electronic configuration is neglected. Typically the electronic structure is only considered in the ab-initio, Tight-Binding and semi-empirical Quantum Mechanics approaches. [10-12]

In this approach, a bond is considered to be the force that connects two atoms (represented as rigid balls) together which can be modeled by a spring. This model depends strongly on the concepts of the bonding and follows the Newtonian laws.

For a nano structure, with a bond between two atoms or molecule, energies due to the bond-stretch, bond-angle bending, dihedral angle torsion, out of plane torsion, van der Waals interactions are considered for small deformations. Using the molecular mechanics approach, nano-materials are modeled in many ways to determine their properties based on the loading conditions or the property to be determined. Some of those are the **stick-spiral model**, **beam-element model** etc.

$$U = U_{\text{stretch}} + U_{\text{bending}} + U_{\text{torsion}} + U_{\text{vdW}} \quad (7)$$

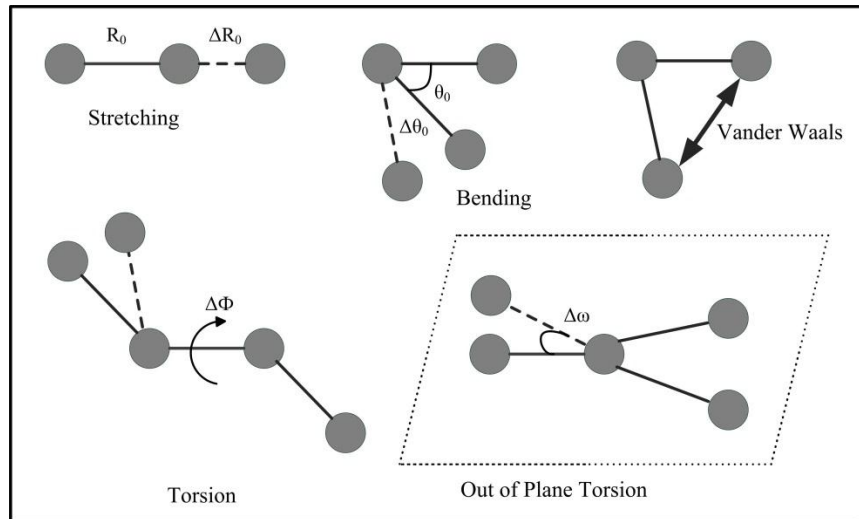
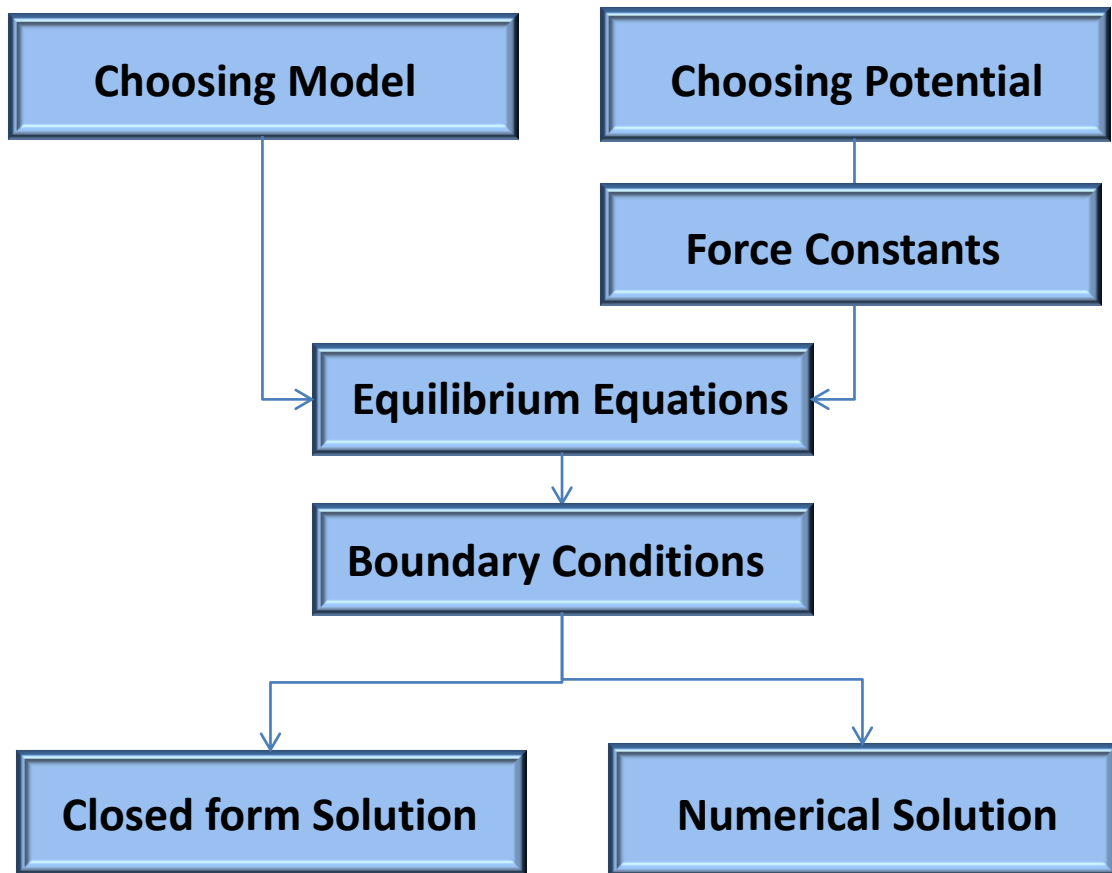


Fig 4: Different atomic interactions due to the mechanical loading on CNTs

Based on the different potential models chosen, each individual term has a specific value which can be used to determine the energy of the system. The properties can be then derived based on these potentials analytically or by employing simulation tools.



Flow Chart 1: Molecular Mechanics approach for evaluation of mechanical properties

2.3.1 CNT size effects on Elasticity

Based on the molecular mechanics approach, considering a stick-spiral model, a closed form solution is found to derive the analytical expression for the elasticity of the carbon nanotube, based on the chirality. We utilized the work done by Tienchong et al.,[10] to verify the effects of the chirality and elasticity on the frequency of the CNTs. This gives an insight of the essentiality of finding the elastic properties, which are very much crucial in the sensor technology field applications. The description about the parameters and complete derivation can be accessed from the actual work of Tienchong et al.[10]

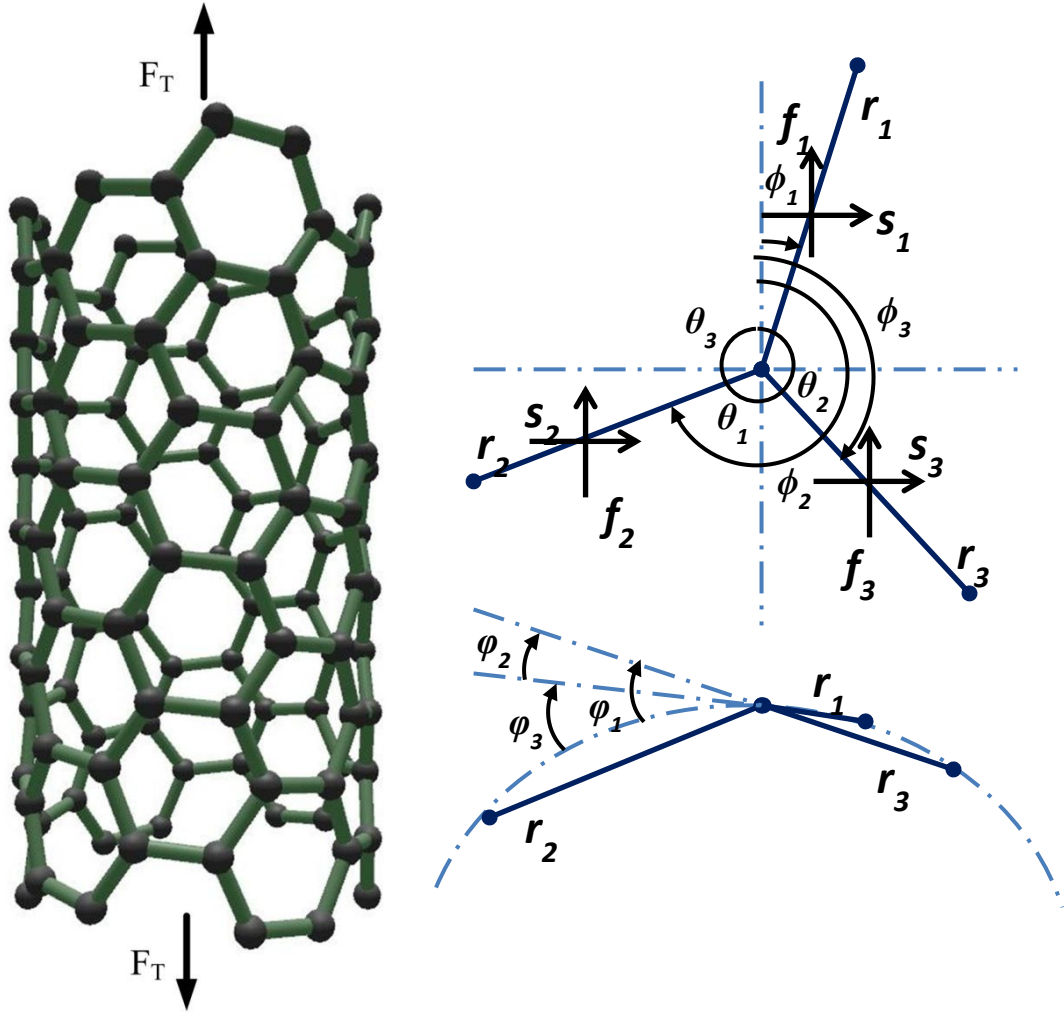


Fig 7: (a) A SWCNT subjected to axial tensile force (b)&(c) geometry and force interactions in side view and top view respectively

The analytical expression for the Young's modulus is given as

$$Y_s = \eta \frac{4\mu K_\rho}{\sqrt{3}(\lambda + 3\mu)} \quad (8)$$

Where η, λ expressions on chiral indices n, m

μ depends on bond length r_i , force constants – K_ρ and K_θ

K_ρ - Axial spring stiffness

K_θ - Spiral spring stiffness

Using this expression the chirality and size dependence of the elasticity of the CNTs were plotted. To calculate the modulus of elasticity, the thickness of the CNTs is considered as 0.08nm in this case. The results clearly show that the dependence of the elasticity of CNTs is more when the diameters are low. The elasticity difference of the two limiting

configurations is almost 70 GPa at 0.4nm diameter range which then drastically reduced to 10 GPa at 1 nm diameter range. At higher diameters (more than 1nm) of the CNTs, the value of the elasticity is almost same for the two configurations.

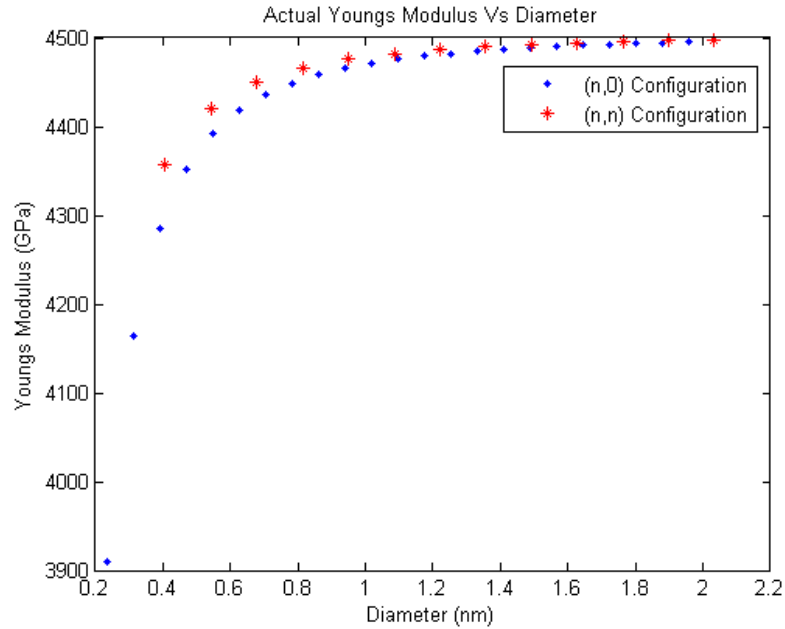


Fig 6: Elasticity vs diameter of CNTs for arm chair and zigzag configurations

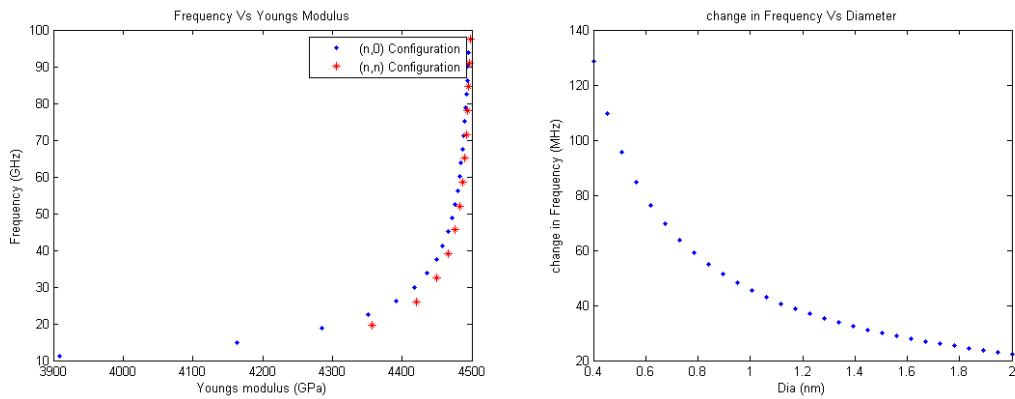


Fig 7: Frequency vs Elasticity and Change in Frequency vs diameter of CNTs for arm chair and zigzag configurations

When these Elasticity values for different configurations are used in calculating the resonance frequency for the model given in the motivation section, it shows the importance of the prediction of elasticity at low diameters. The frequency variations between two limiting configurations (zigzag and arm-chair) is more at smaller diameters, say less than 1 nm, compared to the higher diameters. There is huge frequency difference of 130 MHz at

diameter range of 0.4nm, which reduced to 40MHz for 1 nm diameter range of CNT. Hence the prediction of the size, chirality dependence of the CNTs is of more important in sensor applications in particular.

2.3.2 Stress-Strain Relationship for Armchair CNT

With the stick-spiral model, using the Morse-modified potential model, the stress-strain relationships can be derived from the geometric, force, moment equilibrium equations.

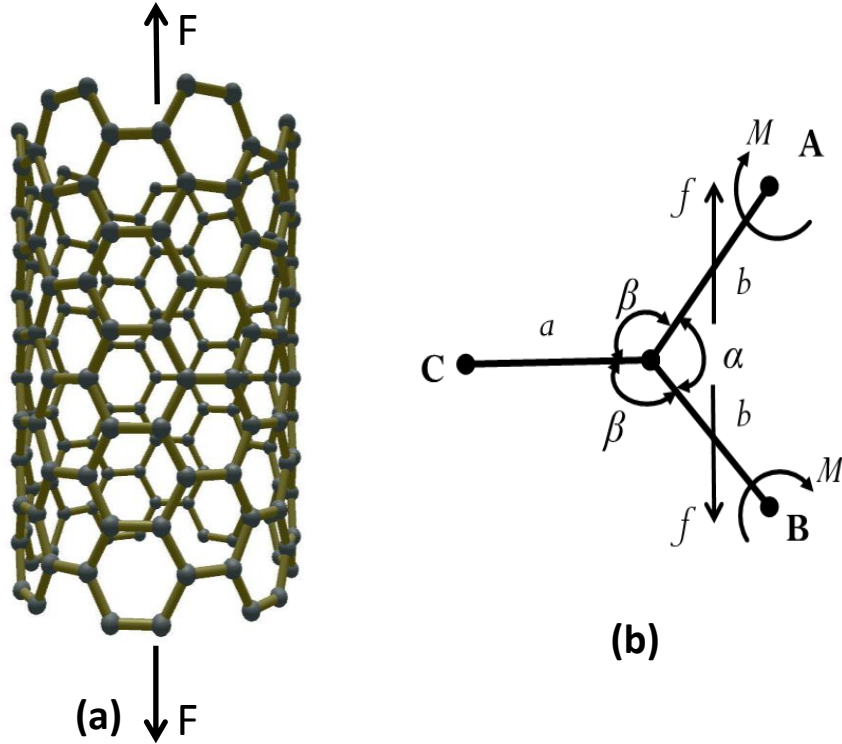


Fig 8: (a) An Armchair SWCNT subjected to axial tensile force (b) Force and Moment interactions in a unit

In this approach, the morse modified potentials are used to evaluate the stick-spiral model, for deriving the stress-strain relationship for both armchair and zigzag configurations. This is a simple static model, which utilizes the geometric, force and moment equilibrium equations for estimating the required properties.

The total energy of the C-C bond can be expressed using the morse modified potentials, neglecting the torsion and dihedral terms as,

$$E_{stretch} = D_e \left\{ \left[1 - e^{-\beta(\Delta r)} \right]^2 - 1 \right\} \quad (9)$$

$$E_{angle} = \frac{1}{2} \cdot k_{\theta} \cdot (\Delta\theta)^2 \cdot \left[1 + k_{sextic} (\Delta\theta)^4 \right] \quad (10)$$

$$Total\ energy = E_{stretch} + E_{angle} \quad (11)$$

From the $E_{stretch}$, the stretch force can be calculated as

$$F(\Delta r) = \frac{d}{d(\Delta r)} E_{stretch} \quad (12)$$

$$F(\Delta r) = 2 \cdot \beta' \cdot D_e \left\{ \left[1 - e^{-\beta'(\Delta r)} \right] \cdot e^{-\beta'(\Delta r)} \right\} \quad (13)$$

Using the E_{angle} term, the moment function interms of $\Delta\theta$

$$M(\Delta\theta) = \frac{d}{d(\Delta\theta)} E_{angle} \quad (14)$$

$$M(\Delta\theta) = k_\theta \cdot \Delta\theta \cdot \left[1 + 3 k_{sextic} (\Delta\theta)^4 \right] \quad (15)$$

For an armchair configuration, the bond lengths are a, b, b and bond angles are α , β , β as shown in the fig 8(b).

By force equilibrium over bond OA,

$$f \cdot \sin\left(\frac{\alpha}{2}\right) = F(\Delta b) \quad (16)$$

Using the moment equilibrium over the bond OA,

$$f \cdot \cos\left(\frac{\alpha}{2}\right) \cdot \frac{b}{2} = M(\Delta\alpha) + M(\Delta\beta) \cdot \cos(\Phi) \quad (17)$$

Φ is the torsion angle between the planes OA-OB and OA-OC

$$\cos(\Phi) = -\frac{\tan\left(\frac{\alpha}{2}\right)}{\tan(\beta)} \quad (18)$$

For arm-chair configuration,

$$\cos(\beta) = \cos\left(\pi - \frac{\pi}{2n_1}\right) \cdot \cos\left(\frac{\alpha}{2}\right) \quad (19)$$

Differentiating the above term we get,

$$-\sin(\beta) \cdot \Delta\beta = -\cos\left(\frac{\pi}{2n_1}\right) \cdot \left(\frac{1}{2}\right) \left[-\sin\left(\frac{\alpha}{2}\right) \right] \Delta\alpha \quad (20)$$

$$\Delta\beta = -\frac{\sin\left(\frac{\alpha}{2}\right)}{2 \cdot \sin(\beta)} \cdot \cos\left(\frac{\pi}{2n_1}\right) \cdot \Delta\alpha \quad (21)$$

Considering, 't' as the thickness of the CNT, the axial stress over the unit cell considered is defined as,

$$Stress = \sigma = \frac{f}{tb \left[1 + \cos\left(\frac{\alpha}{2}\right) \right]} \quad (22)$$

Also the axial strain can be represented as,

$$Axial\ strain = \epsilon = \frac{\Delta b \cdot \sin\left(\frac{\alpha}{2}\right) + \left(\frac{b}{2}\right) \cdot \cos\left(\frac{\alpha}{2}\right) \cdot \Delta\alpha}{b \cdot \sin\left(\frac{\alpha}{2}\right)} \quad (23)$$

The actual work of J. R. Xiao et al,[11] gives a numerical approach in estimating the stress and strains. In this work, we tried to achieve a closed form solution that can give accurate results as compared with the original work.

Using the above set of equations,

$$f = \frac{2 \cdot \beta' \cdot D_e \left\{ \left[1 - e^{-\beta'(\Delta b)} \right] \cdot e^{-\beta'(\Delta b)} \right\}}{\sin\left(\frac{\alpha}{2}\right)} \quad (24)$$

$$f \cdot \cos\left(\frac{\alpha}{2}\right) \cdot \frac{b}{2} = k_{\theta}(\Delta\alpha) \left[1 + 3k_{sextic}(\Delta\alpha)^4 \right] + k_{\theta}(\Delta\beta) \left[1 + 3k_{sextic}(\Delta\beta)^4 \right] \cdot \cos(\Phi) \quad (25)$$

Neglecting the $(\Delta\alpha)^4$ term in the above expression as change in bond angle is very less compared to the bond stretching,

$$\Delta\alpha = \frac{f \cdot \cos\left(\frac{\alpha}{2}\right) \cdot \frac{b}{2}}{k_{\theta}(1-A)} \quad (26)$$

Finally, strain is given as

$$\text{Axial strain} = \frac{K_{\theta}(1-A)(\Delta b) \sin\left(\frac{\alpha}{2}\right) + \left(\frac{b}{2}\right)^2 \cos^2\left(\frac{\alpha}{2}\right) f}{K_{\theta}(1-A)(b) \sin\left(\frac{\alpha}{2}\right)} \quad (27)$$

$$\text{Where } f = \frac{2\beta 1 D_e [1 - e^{-\beta 1 \Delta b}] e^{-\beta 1 \Delta b}}{\sin\left(\frac{\alpha}{2}\right)} \quad (28)$$

$$A = \frac{\sin\left(\frac{\alpha}{2}\right) \cos\left(\frac{\pi}{2n}\right) \cos(\varphi)}{2 \sin(\beta)} \quad (29)$$

$\beta 1$, D_e , K_{θ} are Morse-Modified Potential constants

Δb is the change in bond length of bond 'b' and t is the thickness of the CNT

Applying a bond strain gradually, plot for stress vs strain (fig 9) was obtained for armchair configuration using MATLAB programming, for different diameters that change due to chirality index number n.

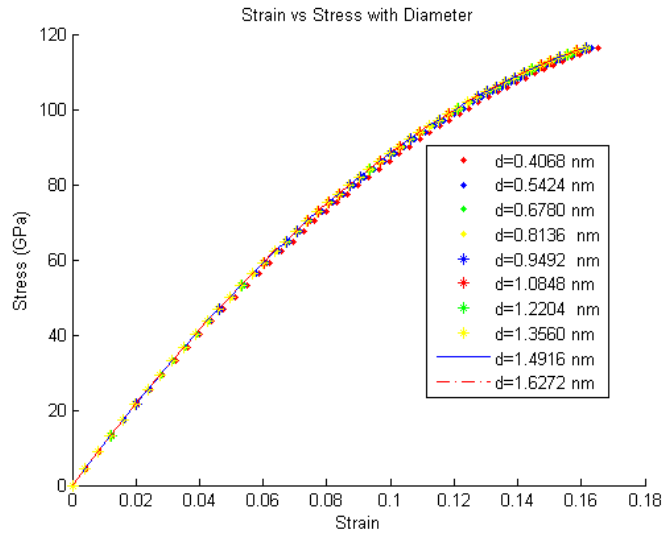


Fig 9: Non-Linear stress strain relationship for Arm chair configurations of different diameters

As seen from the plot, the stress-strain relationship is linear until the strain of 0.08 and then non-linearity starts up. With the increasing strains after 0.1, the non-linear effects are more rapid. It can also be noted that the behavior of the armchair configuration is almost similar for almost all diameters and hence the elastic properties are insensitive to the size of the armchair CNTs. However, there will be slight variation in the elastic properties at higher strains and is slightly dependent on the diameter, more particularly in the non-linear zone.

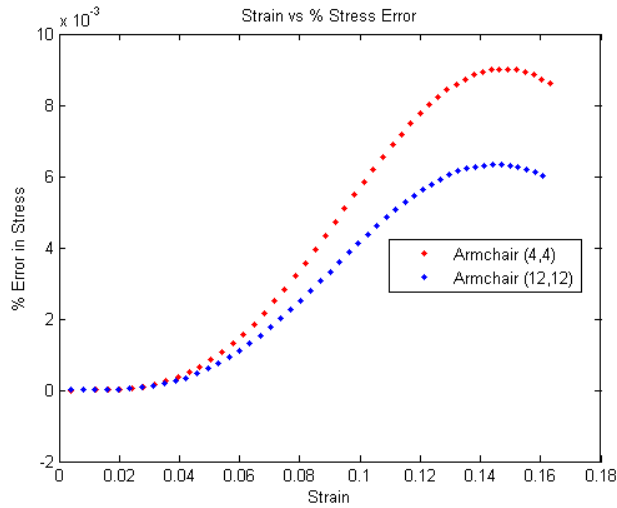
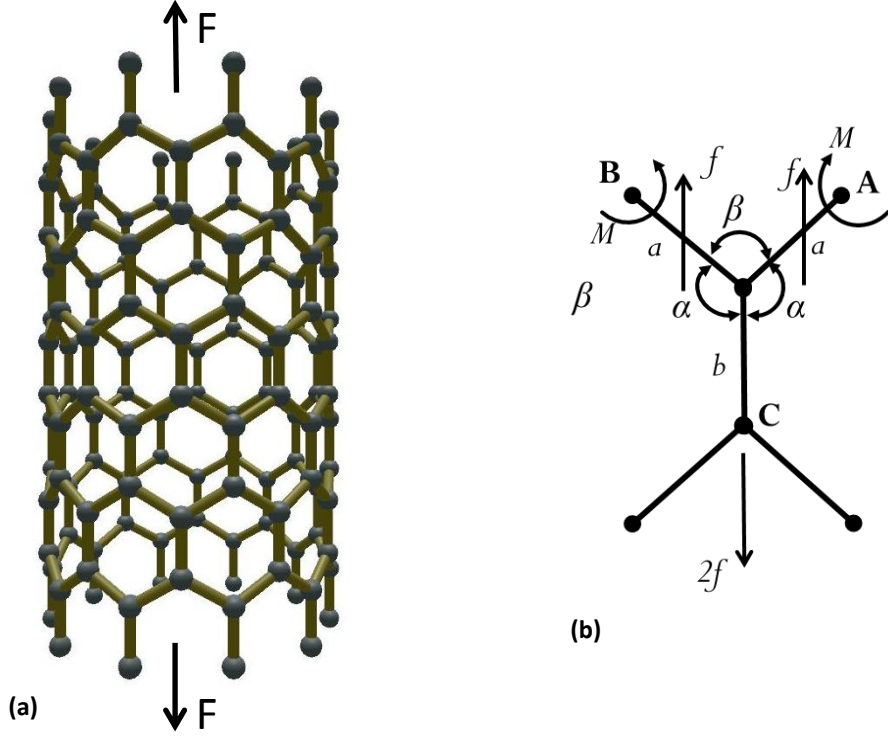


Fig 10(a): % Error in stress for (4,4) and (12,12) arm chair configurations w.r.t J.R. Xiao etal

The present work is compared with the work of Xiao etal,[11] and the results are very much satisfactory. The error in the stress-strain relationship for the two models is increases with the increasing Chirality index of the armchair CNTs and however the % error as seen in fig15 is almost negligible.

2.3.3 Stress-Strain Relationship for zigzag CNT

Using the same approach for the zigzag configuration, as discussed earlier for the arm-chair configuration, we deduced a closed form solution for stress-strain relationship.



**Fig 10: (a) Zigzag SWCNT subjected to axial tensile force
(b) Force and Moment interactions in a unit**

Here, the bond lengths are considered as a , a , b and bond angles are taken as α , α , β as shown in the fig 10(b). Due to the geometric differences between the considered unit cells for analysis, the torsion angle is given as,

$$\cos(\Phi) = -\frac{\tan\left(\frac{\beta}{2}\right)}{\tan(\alpha)} \quad (30)$$

Change in bond angle $\Delta\beta$ is expressed as,

$$\Delta\beta = -\frac{2\cos(\alpha)}{\cos\left(\frac{\beta}{2}\right)} \cdot \cos\left(\frac{\pi}{n_1}\right) \cdot \Delta\alpha \quad (31)$$

Now f is deduced as,

$$f = \frac{F(\Delta a)}{\cos(\pi - \alpha)} \quad (32)$$

From the force and moment equilibrium equations, over the bond OA,

$$F(\Delta b) = 2f \quad (33)$$

$$f \cdot \frac{a}{2} \cdot \sin(\pi - \alpha) = M(\Delta a) + M(\Delta\beta) \cdot \cos(\Phi) \quad (34)$$

Now, stress and strain are given as,

$$\sigma = \frac{f}{t \cdot a \cdot \sin(\pi - \alpha)} \quad (35)$$

$$\epsilon = \frac{\Delta b + \Delta a \cdot \cos(\pi - \alpha) + a \cdot \sin(\pi - \alpha) \cdot \Delta \alpha}{b + a \cdot \cos(\pi - \alpha)} \quad (36)$$

Using the above equations, we get,

$$f \left(\frac{a}{2} \right) \cdot \sin(\pi - \alpha) = k_{\theta} (\Delta \alpha) [1 + C + D(\Delta \alpha)^4] \quad (37)$$

$$\frac{2 \cos(\alpha) \cdot \cos\left(\frac{\pi}{n_1}\right) \cdot \cos(\Phi)}{\cos\left(\frac{\beta}{2}\right)} = C \quad (38)$$

$$3 k_{\text{sextic}} \cdot \left[1 + 16 \frac{\cos^4(\alpha)}{\cos^4\left(\frac{\beta}{2}\right)} \cdot \cos^4\left(\frac{\pi}{n_1}\right) \cdot \cos(\Phi) \right] = D \quad (39)$$

Neglecting the $(\Delta \alpha)^4$ term in the above expression, $\Delta \alpha$ can be derived as,

$$\Delta \alpha = \frac{f \left(\frac{a}{2} \right) \cdot \sin(\pi - \alpha)}{k_{\theta} (1 + C)} \quad (40)$$

Using $\Delta \alpha$ in the stress and strain expression, we get

$$\text{strain} = \frac{K_{\theta} (1 + C) (\Delta b + \Delta a \cos(\pi - \alpha)) + \left(\frac{a^2}{2} \right) \sin^2(\pi - \alpha) f}{K_{\theta} (1 + C) (b + a \cos(\pi - \alpha))} \quad (41)$$

$$\text{Where } f = \frac{2\beta 1 D e [1 - e^{-\beta 1 \Delta a}] e^{-\beta 1 \Delta a}}{\cos(\pi - \alpha)} \quad (42)$$

$$C = \frac{2 \cos(\alpha) \cos\left(\frac{\pi}{n_1}\right) \cos(\varphi)}{2 \cos\left(\frac{\beta}{2}\right)} \quad (43)$$

$\beta 1$, $D e$, K_{θ} are Morse-Modified Potential constants

Δa is the change in bond length of bond 'a', Δb is the change in bond length of bond 'b' and t is the thickness of the CNT. Δb can be calculated using the above expression for various Δa values with the below expression.

$$\left[1 - e^{-\beta'(\Delta b)} \right] \cdot e^{-\beta'(\Delta b)} = \frac{2 \cdot \left[1 - e^{-\beta'(\Delta a)} \right] \cdot e^{-\beta'(\Delta a)}}{\cos(\pi - \alpha)} \quad (44)$$

For small change in bond strains, the stress and strain behavior of the unit cell is calculated using the above analytical expressions on MATLAB over different diameters of zigzag configuration (fig 11).

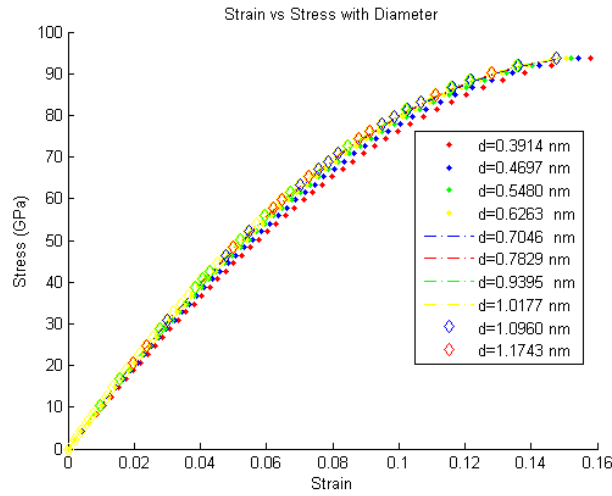


Fig 11: Non-Linear stress strain relationship for zigzag chair configurations of different diameters

Unlike the armchair configuration, the behavior of the zigzag CNTs are dependent on their diameters and this effect is more in the non-linear zone at higher strains. Also the linear relationship exist only upto 0.06 strain and there after the non-linear effects are more dominating. However the linearity strain limit increases with the increasing size of the zigzag configuration. Finally, it is evident that the zigzag CNTs are sensitive to their chirality index number.

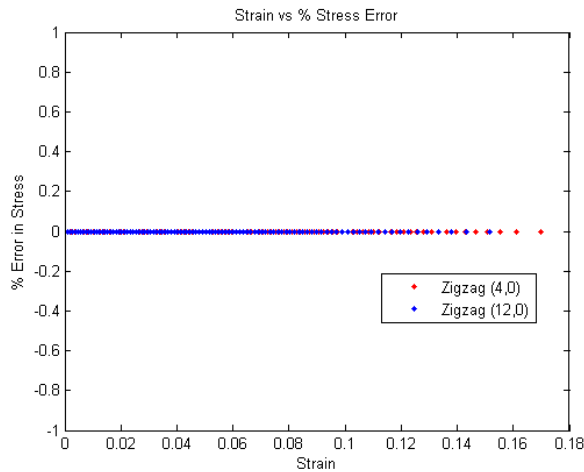


Fig 11 (a): % Error in stress for (4,0) and (20,0) configurations w.r.t J.R. Xiao etal

When compared with the results of the existing work by Xiao etal,[11] the results are very much coinciding and the effect of neglecting fourth order term of change in bond angle is nil.

Chapter 3

Numerical Analysis of Carbon Nanotube

3.1 Beam Element Modeling of CNT

The beam element model is also a molecular mechanics approach which falls under the structural mechanics sub-section. Unlike the stick-spiral model, this model can take care of the torsion effects in the C-C bond. This method can be effectively used for analyzing the CNT structure by combining with the FEM approach on a readily available analysis packages such as ANSYS, ABAQUS etc. [14]

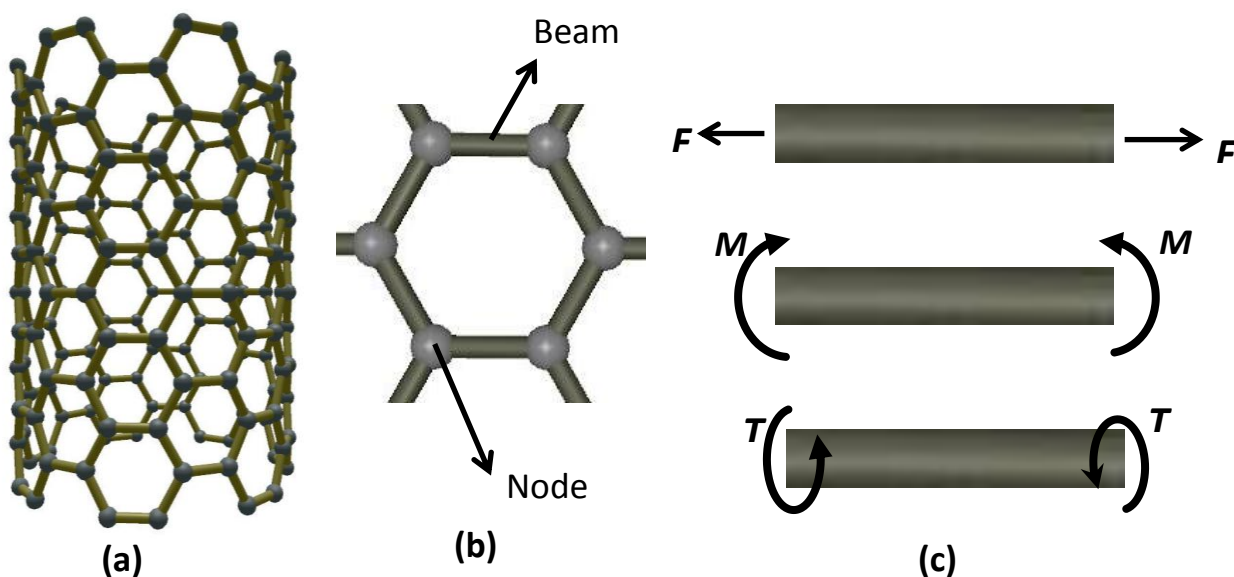


Fig 12 : (a) CNT Structure
(b) A unit hexagon ring with beam elements and nodes
(c) Stretching, Moment and Torque Interactions on the beam element

The basis of this method is derived from the energy equivalence of the structural and molecular mechanics. As per molecular mechanics approach the main contributions for a Covalent bond under small deformations are -

Bond stretch interaction energy

$$U_r = \frac{1}{2}k_r(\Delta r)^2 \quad (45)$$

Bond angle bending energy

$$U_\theta = \frac{1}{2}k_\theta(\Delta\theta)^2 \quad (46)$$

Dihedral angle Torsional energy

$$U_T = \frac{1}{2}k_T(\Delta\phi)^2 \quad (47)$$

For the classical structural mechanics approach the strain energies for a beam structure are -

Under pure axial Force

$$U_A = \frac{EA}{2L}(\Delta L)^2 \quad (48)$$

Under pure bending

$$U_M = \frac{EI}{2L}(2\alpha)^2 \quad (49)$$

Under pure torsion

$$U_T = \frac{GJ}{2L}(\Delta\beta)^2 \quad (50)$$

Therefore a direct relationship between the parameters of the molecular mechanics and structural mechanics can be established as –

$$\frac{EA}{L} = k_r \quad \frac{EI}{L} = k_\theta \quad \frac{GJ}{L} = k_T \quad (51)$$

For a circular beam section with diameter ‘d’, the linkage parameters can be obtained as

$$d = 4\sqrt{\frac{k_\theta}{k_r}} \quad E = \frac{k_r^2 L}{4\pi k_\theta} \quad G = \frac{k_r^2 L k_T}{8\pi k_\theta^2} \quad (52)$$

Using C-C bond length of 0.1421nm as L and the force constants of $k_r = 6.52 \times 10^{-7} \text{ N nm}^{-1}$, $k_\theta = 8.76 \times 10^{-10} \text{ N nm rad}^{-2}$, $k_T = 2.78 \times 10^{-10} \text{ N nm rad}^{-2}$

The final values for the beam element to be used in FEM procedure are evaluated as $d = 0.147 \text{ nm}$, $E = 5.49 \text{ TPa}$, $G = 0.871 \text{ TPa}$ [14]

3.2 Modeling tools and approach for ANSYS analysis

The modeling of the CNTs in ANSYS APDL needs well-defined nodal and elemental information. For this purpose, a initial set of 3 rows of atomic points in xyz coordinate frame are pulled from the Nanotube Modeler (Trial Version) software from JCrystalSoft. Then MATLAB coding is done to generate the required number of points based on the length and chirality of the CNTs. The nodal points generated are in a sequential order for each row. The program also generates the elemental information as per the structures of the armchair and zigzag configurations. Also the programs are written to generate the graphene nodal and elemental data for a given length and width. The main advantage with the MATLAB programming is that the codes are capable enough to write the nodal and elemental data on the text files in the format as required for the ANSYS APDL command

line prompt. The only parameters that are required are the index number (n) and the L/D ratio. For the analysis of CNTs, the ANSYS APDL 13.0 (non-commercial version for educational purpose) has been utilized. ANSYS has been extensively used for the static and modal analysis of the armchair, zigzag CNT configurations and Graphene. In ANSYS two node beam element 188 is used for CNT analysis which has a 6 degrees of freedom on each node. This element has the capability to capture the non-linearity effectively with the NLGEOM, ON option and is well-suited for linear, large rotation, and/or large strain nonlinear applications. The non-linear element properties needs to be plugged into the ANSYS for this element in the material properties. Care needs to be taken that the initial slope of the non-linear stress strain data is equal to the initial elasticity value entered.

From the Morse modified potential, the force vs the bond strain effect is introduced in to the beam element by calculating the stress-strain relationship for the beam dimensions. The below force function in terms of the initial and final bond distance is derived from the Morse stretch potential function. [16]

$$F_{\text{Morse}} = 2\beta_1 D e [1 - e - \beta_1(r - r_0)] e - \beta_1(r - r_0) \quad (53)$$

Where $\beta_1, D e$ are the Morse modified potential function constants and r, r_0 are the final and initial distance between two atoms. The bond strain is thus calculated as

$$\text{Bond Strain}(\varepsilon_b) = \frac{r - r_0}{r_0} \quad (54)$$

Using this force function, the stress generated in the beam element is calculated against the bond strains. The required dimensions for calculating the stress and strain in the beam element are already available from the previous section. This stress-strain relationship is used in defining the non-linearity for the beam element in the ANSYS package. This step is very much essential to tap the non-linear effects in the CNTs.

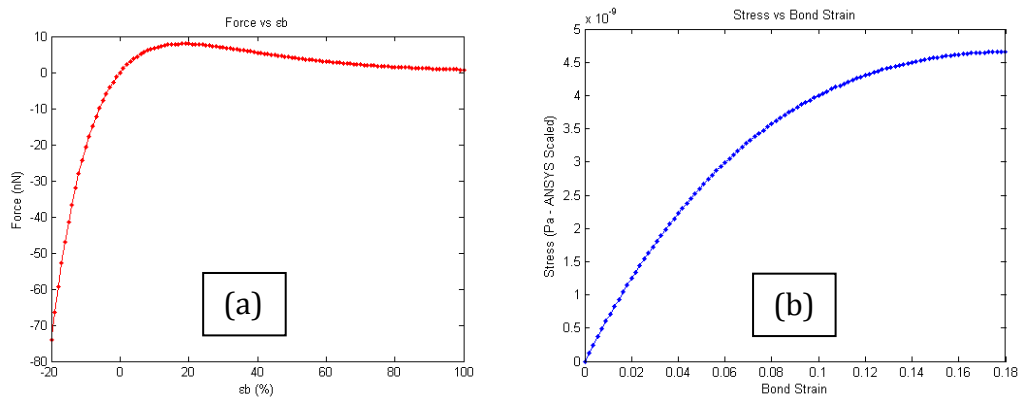


**Fig 13: (a) Force vs ε_b plot for Morse Modified Potential
(b) Stress vs strain relationship used for the ANSYS beam element**

The Density of the beam element is necessary for the Modal Analysis of the CNT/Graphene structures in ANSYS. As the structure of the CNT/Graphene is a honey comb structure, each carbon atom is shared between three beam elements. The effective mass contribution of one carbon atom on each beam is one-third of its mass (mass of carbon atom is 19.9×10^{-27} Kg). As a beam element contains two carbon atoms at its nodal points, the overall mass of the beam element is two-third of a carbon atom. With the earlier calculated beam dimensions, the effective density of the beam element is found to be $5.501 \times 10^3 \text{ Kg m}^{-3}$.

3.3 Scaling Factors and details of CNT/Graphene Models on ANSYS

For modeling the CNTs with nano dimensions, a sufficient scaling factor needs to be taken for each of the parameters for the input and output of the ANSYS simulations.

Sl. No.	Parameter	True Value Units	True Value	Ansys Value	Scaling Factor ***
1	Diameter (Beam Element)	m	1.47×10^{-10}	1.47	10^{-10}
2	Length (Beam Element)	m	1.42×10^{-10}	1.421	10^{-10}
3	Stress (Beam Element)	N/m ²	1.00×10^{10}	1.00×10^{-10}	10^{20}
4	Strain (Beam Element)	m/m	1.00	1	1
5	Elasticity (Beam Element)	N/m ²	5.49×10^{12}	5.49×10^{-8}	10^{20}
6	Rigidity (Beam Element)	N/m ²	8.71×10^{11}	8.71×10^{-9}	10^{20}
7	Density (Beam Element)	Kg/m ³	5.501×10^3	5.501×10^{-27}	10^{30}
8	Force on CNT/Graphene	N	1.00	1.00	1
9	Displacement on CNT/Graphene	m	1.00×10^{-10}	1	10^{-10}
10	Frequency of CNT/Graphene	Hz	1.00	1×10^{-5}	10^5

*** Multiply the Ansys Value with Scaling Factor to get True value
 True Value = Ansys Value x Scaling Factor

Table 1: Table with the details of the Scaling factors for different parameters for simulating CNT/Graphene in ANSYS

The information on the dimensions, number of nodes, number of elements and the maximum displacement applied for various configurations of CNTs and Graphene are listed in the below table.

Sl. No.	Structure	Configuration	Diameter/Width (A)	Thickness (A)	Length (A)	No. of Nodes	No. of Elements	Max. Disp (A)
1	CNT	Armchair (5,5)	6.7848	3.4	80	660	980	12.5
2	CNT	Armchair (8,8)	10.8556	3.4	129.2	1696	2528	20
3	CNT	Armchair (10,10)	13.5695	3.4	161.2	2640	3940	25
4	CNT	Zigzag (8,0)	6.2675	3.4	77.45	592	880	12
5	CNT	Zigzag (10,0)	7.8344	3.4	94.5	910	1350	15
6	CNT	Zigzag (16,0)	12.535	3.4	154.17	2352	3504	24
7	Graphene	Armchair (5,5)	24.2	3.4	80	804	1160	12.5
8	Graphene	Armchair (8,8)	36	3.4	129.2	1926	2817	20
9	Graphene	Armchair (10,10)	44	3.4	159	2882	4235	25
10	Graphene	Zigzag (8,0)	19.69	3.4	79.6	646	922	12
11	Graphene	Zigzag (10,0)	24.61	3.4	96.62	966	1392	15
12	Graphene	Zigzag (16,0)	39.38	3.4	156.3	2442	3572	24

Table 2: The details of the different configurations of CNTs/Graphenes used for simulation in ANSYS

3.4 Comparison of the ANSYS simulation results

The CNTs and graphene are loaded gradually with displacements by fixing one end; the reaction force for each loading is taken from the ANSYS to calculate the stress on the CNTs/graphene. The stress-strain relationships are obtained for each of the configurations and are plotted as below. [15] [16]

The armchair CNTs (fig.14) have a linear region upto a strain limit of 0.08 and the non-linearity increases rapidly after 0.1 strain. The size effect on the elastic properties of the armchair configuration CNT is almost negligible. The effect of diameter comes into play at larger strain rates and however, the effects are negligible.

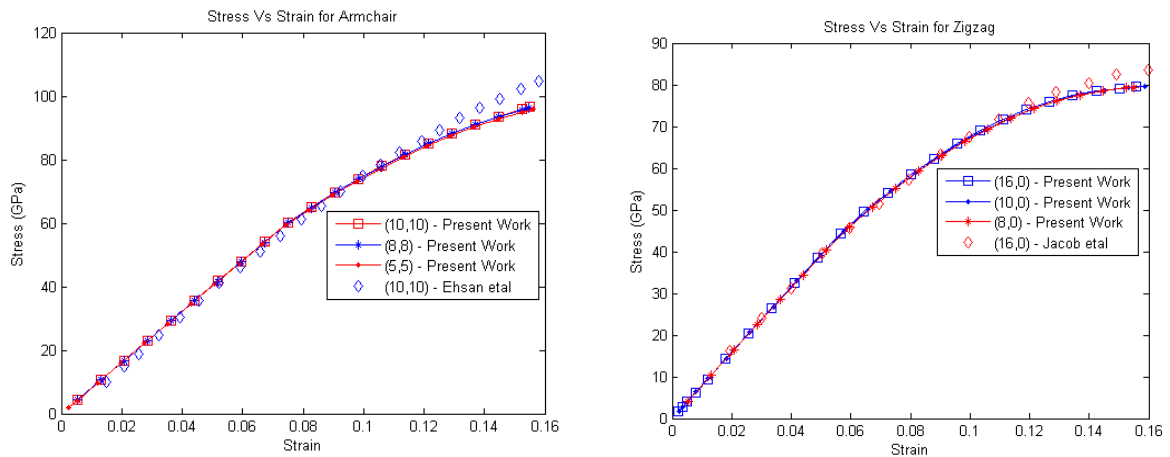


Fig 14: Stress Vs Strain plots for armchair and zigzag CNTs

On the other hand, the zigzag configuration (fig.14) is relatively sensitive to the size of the CNT. The diameter effects on the behavior of the zigzag CNTs are more at larger strain values. The linear region of the zigzag configuration can be observed until the 0.06 strain limit and then it becomes rapid after 0.08 strain value.

As the graphene sheets are two dimensional structures, the size effects for both the armchair and zigzag configurations are negligible (fig 15). The stress-strain relationship is linear for almost 0.08 strain for the armchair graphene sheet, whereas for zigzag configuration the linear strain limit is 0.06. The effect of non-linearity is predominant after 0.1 strain limit for the armchair configuration and for zigzag the effect is active from 0.08 strain value.

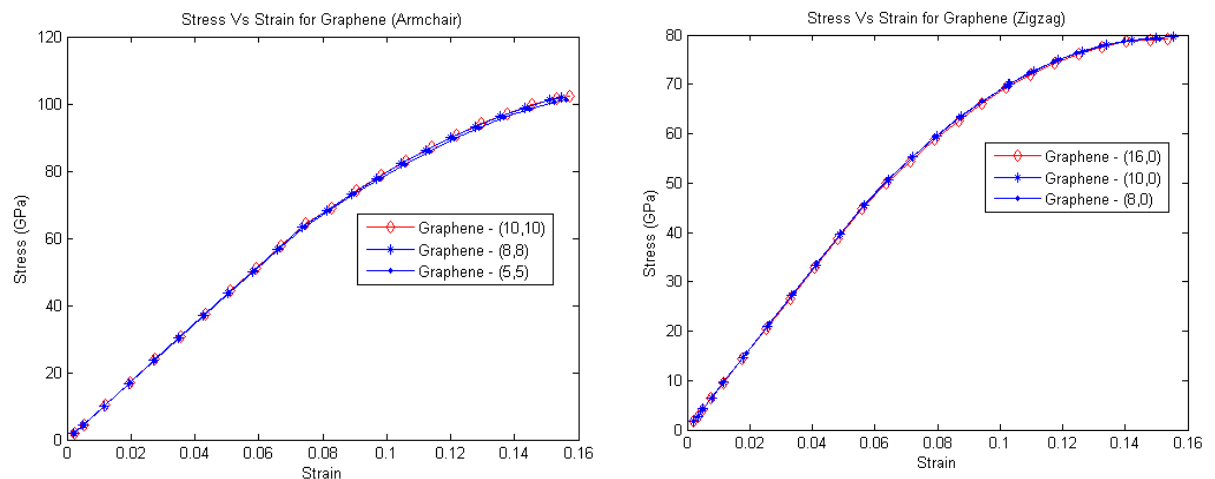


Fig 15: Stress vs Strain plot for different Graphene Configurations

Comparing the stress-strain behavior of the two configurations of CNTs and the corresponding graphene configurations, the effect of rolling graphene into CNT can be analyzed. Here it can be noticed that the deviation in the behavior is more for armchair CNT and Graphene configuration. Also the effect of rolling in the tensile behavior increases with increasing strain rates for the armchair configuration. However there is no significant effect of rolling on the zigzag configuration of the CNTs.

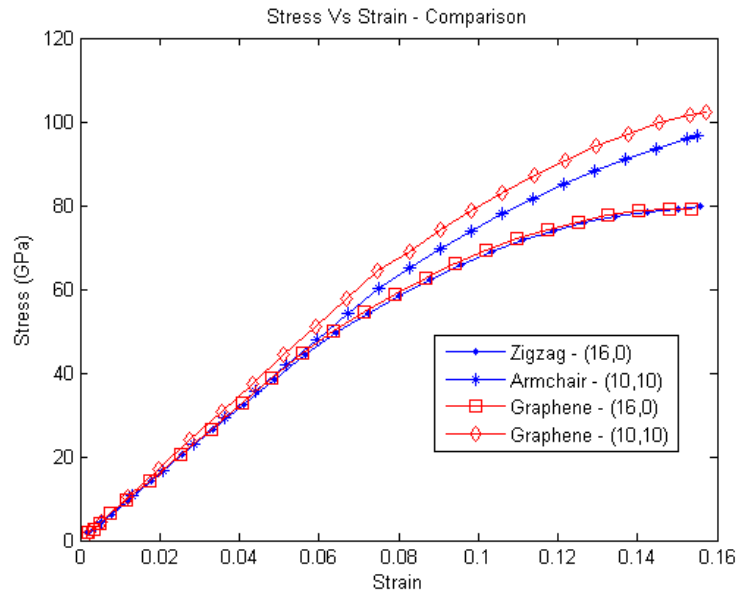


Fig 16: Stress vs Strain comparison plot for Armchair, Zigzag and Graphene Configurations

The ANSYS model is compared with the previous stick-spiral model, and a large variation in stress-strain behavior can be observed. The values of stress for a given strain for ANSYS model are lesser compared to the stick spiral model, as the analysis is stick-spiral model is based on a single unit and the results are not capable enough to capture the behavior of the overall structure. As the ANSYS model utilizes the FEM background, the effects of the neighboring atoms and bonds are nicely simulated. However the ANSYS model also needs to be improvised for better accuracy in results.

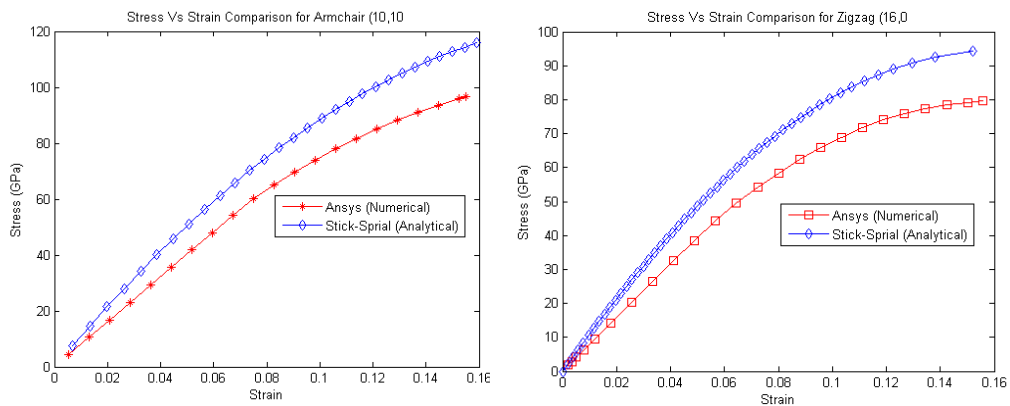


Fig 17: Stress vs Strain comparison plot for Stick-spiral and Beam Element models

The fig.18 shows the beginning of the decrease in the instantaneous elasticity derived from the stress-strain behavior of the armchair and zigzag configurations. The reduction in elasticity is sudden and drastic in case of zigzag configuration. Also the initial elastic modulus of 0.8 TPa for the CNTs matches with most of the available literatures.

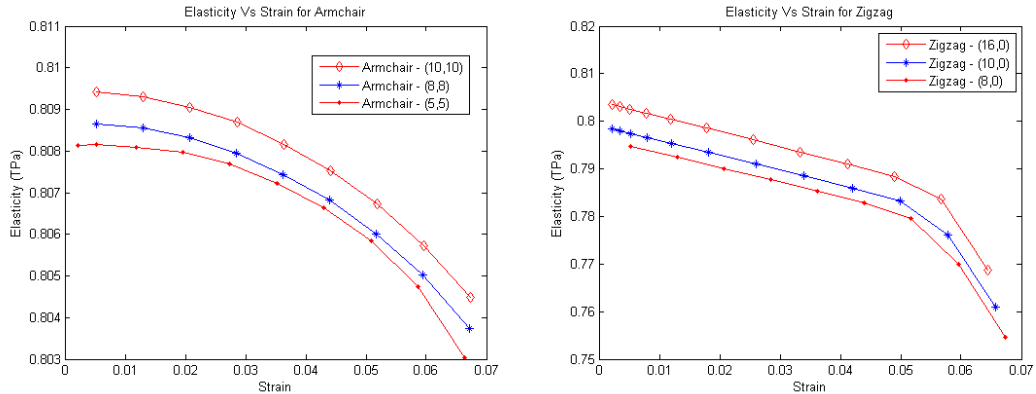


Fig 18: Elasticity variation in Armchair and Zigzag CNTs with Strain

The force vs displacement for each of the configurations of CNTs and graphene are plotted in the fig.19. These plots give a brief overview on the stiffness changes in CNTs and graphene at various loading conditions. These properties are very much essential in deriving the non-linear stiffness coefficient for dynamic analysis of CNTs and graphene.

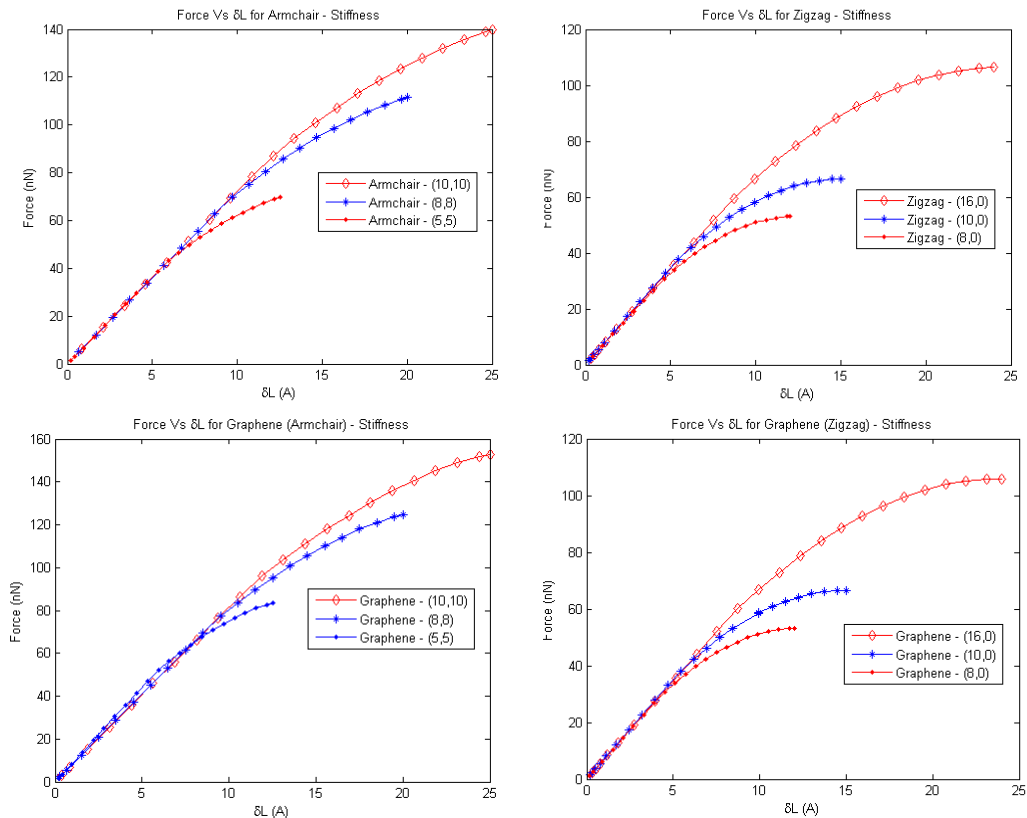


Fig 19: Force Vs Displacement plots for various configurations of CNTs and Graphene

Chapter 4

Modal Analysis of CNTs

4.1 Continuum Models for Modal Analysis

The CNT/Graphene models are also subjected to the Modal Analysis in ANSYS and the results are compared with that of the available continuum models of CNTs for fixed and cantilever end conditions.

Fixed Beam subjected to free vibrations with zero axial load:

Considering the CNT as a hollow cylindrical structure, using the continuum models, for a beam subjected to axial load P, the governing equation for the lateral vibrations is given as – [4]

$$EI \frac{\partial^4 w}{\partial x^4} + \rho A \frac{\partial^2 w}{\partial t^2} - P \frac{\partial^2 w}{\partial x^2} = 0 \quad (55)$$

Where $A = 2\pi R_0 t_0$, $I = \pi R_0 t_0 (4R_0^2 + t_0^2)/4$, R_0 , t_0 are the radius and thickness of the CNT respectively

The natural frequency of the beam without pre-strain is obtained as –

$$f_p = \frac{4.73^2}{2\pi L^2} \sqrt{\left(\frac{EI}{\rho A}\right)} \quad (56)$$

Cantilever Beam subjected to free vibrations:

For a cantilever beam subjected to free vibrations, the governing equation is given as –

$$EI \frac{\partial^4 w}{\partial x^4} - \omega^2 m w = 0 \quad (57)$$

The first natural frequency of the beam is obtained as –

$$f_p = \frac{1.875^2}{2\pi L^2} \sqrt{\left(\frac{EI}{\rho A}\right)} \quad (58)$$

The modal frequencies obtained from the ANSYS simulations are compared with the theoretical natural frequencies calculated from the above formulae are listed in the tables 3 and 4. The results are satisfactorily matching with the continuum models at higher L/D ratios for all the configurations in both fixed-fixed and cantilever end conditions.

Sl. No.	Configuration	Diameter (A)	Thickness (A)	L/D Ratio	Elasticity (Gpa)	Theoretical Frequency (GHz)	ANSYS Frequency (GHz)	% Error
1	Armchair (10,10)	13.5695	3.4	12	809.42	125.98	114.02	9.49
2	Armchair (10,10)	13.5695	3.4	10	809.42	181.41	156.00	14.01
3	Armchair (10,10)	13.5695	3.4	8	809.42	283.45	233.52	17.61
4	Armchair (10,10)	13.5695	3.4	6	809.42	503.91	372.90	26.00
5	Zigzag (16,0)	12.535	3.4	12	803.51	136.56	115.37	15.52
6	Zigzag (16,0)	12.535	3.4	10	803.51	196.65	160.13	18.57
7	Zigzag (16,0)	12.535	3.4	8	803.51	307.26	235.44	23.37
8	Zigzag (16,0)	12.535	3.4	6	803.51	546.25	375.04	31.34

Table 3: Comparison of the First natural frequency for different configurations from ANSYS simulations w.r.t. Continuum Model (Fixed beam)

Sl. No.	Configuration	Diameter (A)	Thickness (A)	L/D Ratio	Elasticity (Gpa)	Theoretical Frequency (GHz)	ANSYS Frequency (GHz)	% Error
1	Armchair (10,10)	13.5695	3.4	12	809.42	19.80	19.50	1.51
2	Armchair (10,10)	13.5695	3.4	10	809.42	28.51	27.51	3.49
3	Armchair (10,10)	13.5695	3.4	8	809.42	44.54	43.54	2.26
4	Armchair (10,10)	13.5695	3.4	6	809.42	79.18	76.39	3.52
5	Zigzag (16,0)	12.535	3.4	12	803.51	21.46	19.55	8.89
6	Zigzag (16,0)	12.535	3.4	10	803.51	30.90	27.94	9.57
7	Zigzag (16,0)	12.535	3.4	8	803.51	48.28	43.12	10.70
8	Zigzag (16,0)	12.535	3.4	6	803.51	85.84	74.79	12.87

Table 4: Comparison of the First natural frequency for different configurations from ANSYS simulations w.r.t. Continuum Model (Cantilever beam)

4.2 Bending Modes and Fundamental Frequencies

The first three bending mode frequencies for different end conditions, at different L/D ratios for armchair and zigzag configuration of CNTs are plotted as below. [17] [18]

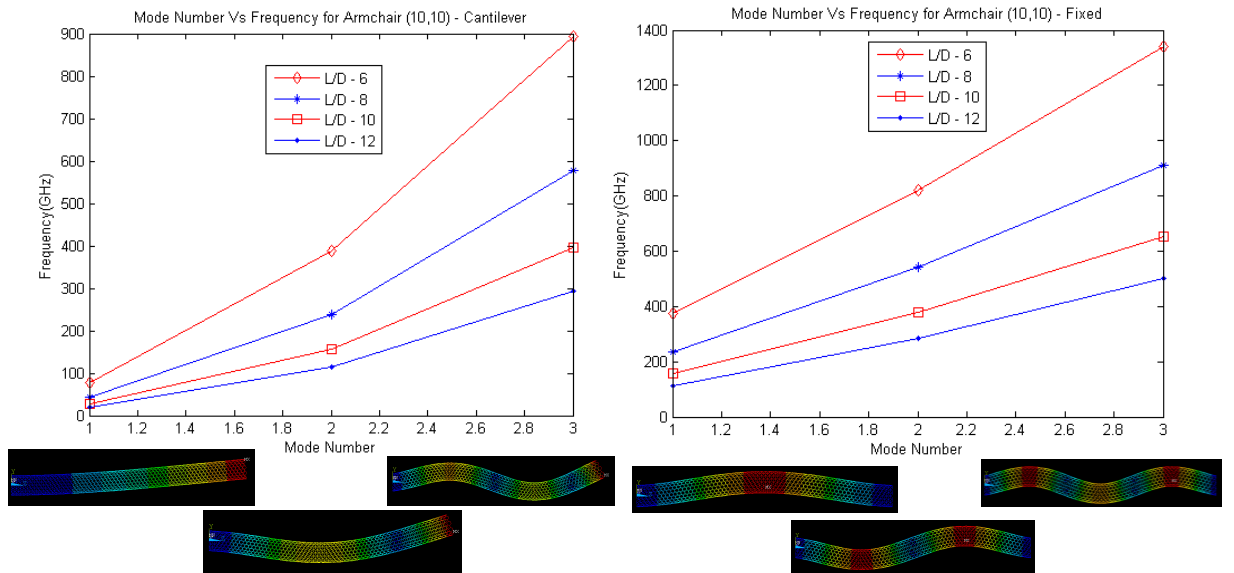


Fig 21: First three bending mode frequencies for cantilever and fixed Armchair configuration over various L/D Ratios

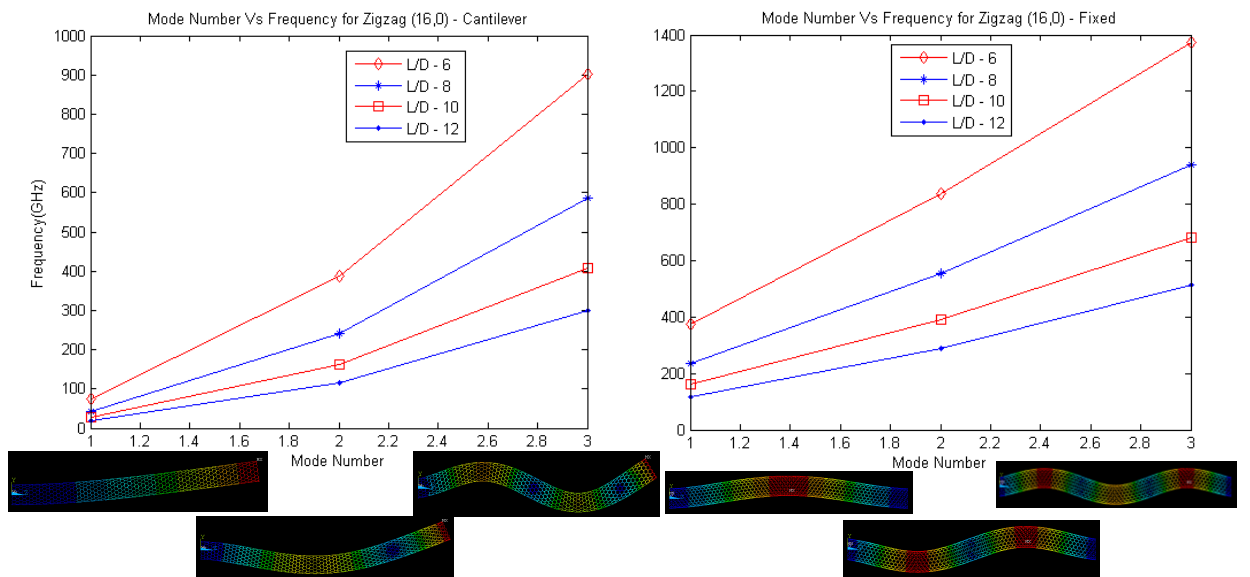


Fig 22: First three bending mode frequencies for cantilever and fixed Zigzag configuration over various L/D Ratios

From the fig. 21 & fig. 22, it is evident that the frequencies for each mode are higher at lower L/D ratios. Even the subsequent ratios for the higher modes w.r.t to the corresponding fundamental frequencies are also well maintained for different L/D ratios of different configurations of CNT under both cantilever and fixed end conditions.

The first fundamental frequency for bending for different end conditions, over the different L/D ratios for armchair and zigzag configuration of CNTs are plotted as below.

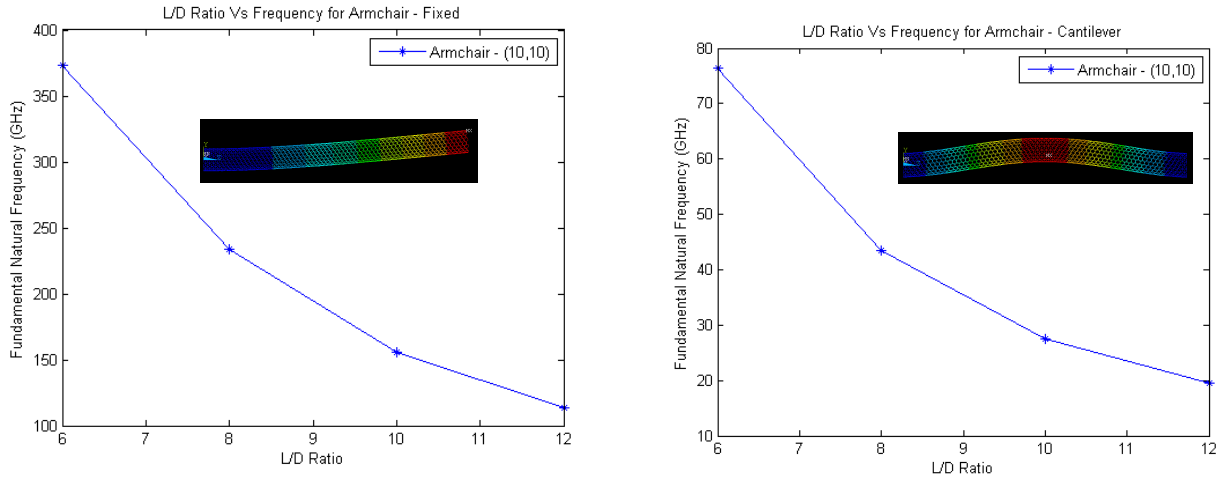


Fig 23: First fundamental frequency for bending mode for Armchair configuration in cantilever and fixed conditions w.r.t L/D Ratio

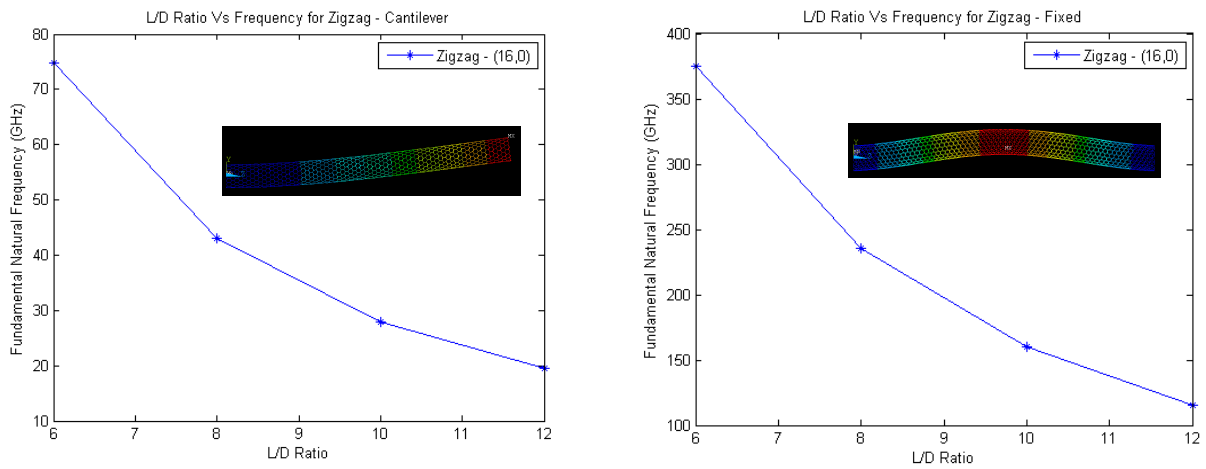
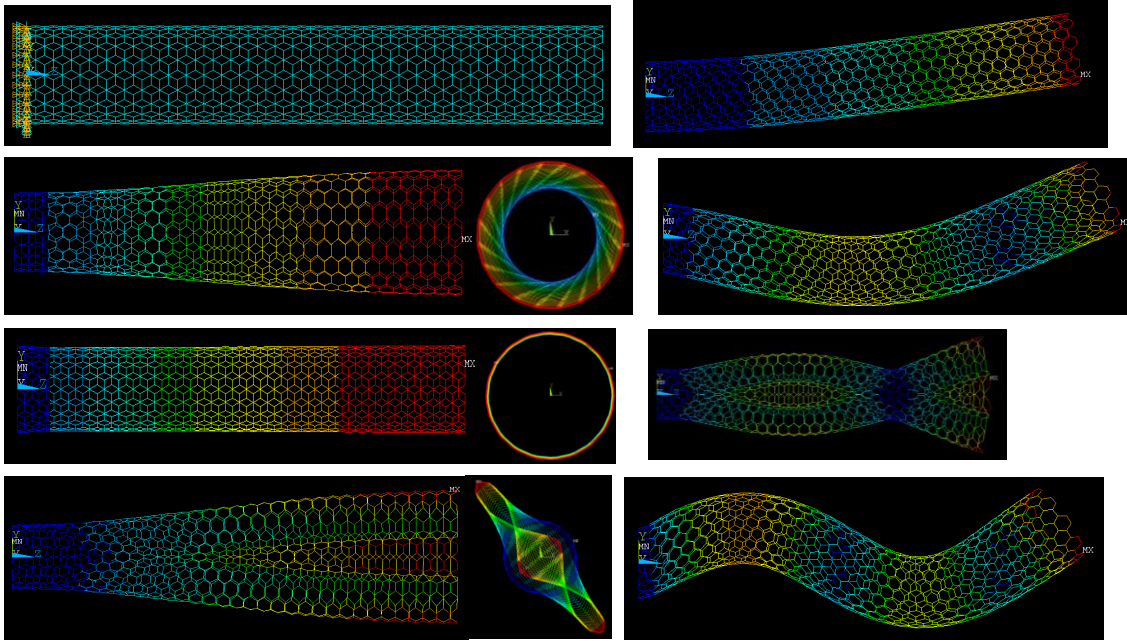


Fig 24: First fundamental frequency for bending mode for Zigzag configuration in cantilever and fixed conditions w.r.t L/D Ratio

From the fig. 23 & fig. 24, for each configuration under different end conditions, the fundamental frequencies are increasing with decreasing L/D ratios. The plots obtained above will have a good curved shape if the analysis is conducted for the intermediate ratios of the L/D ratios.

4.3 Different modes of vibrations



**Fig 25: Different modes of vibration for Cantilevered Armchair configuration with L/D 6 ratio
Bending, Torsion, Warping**

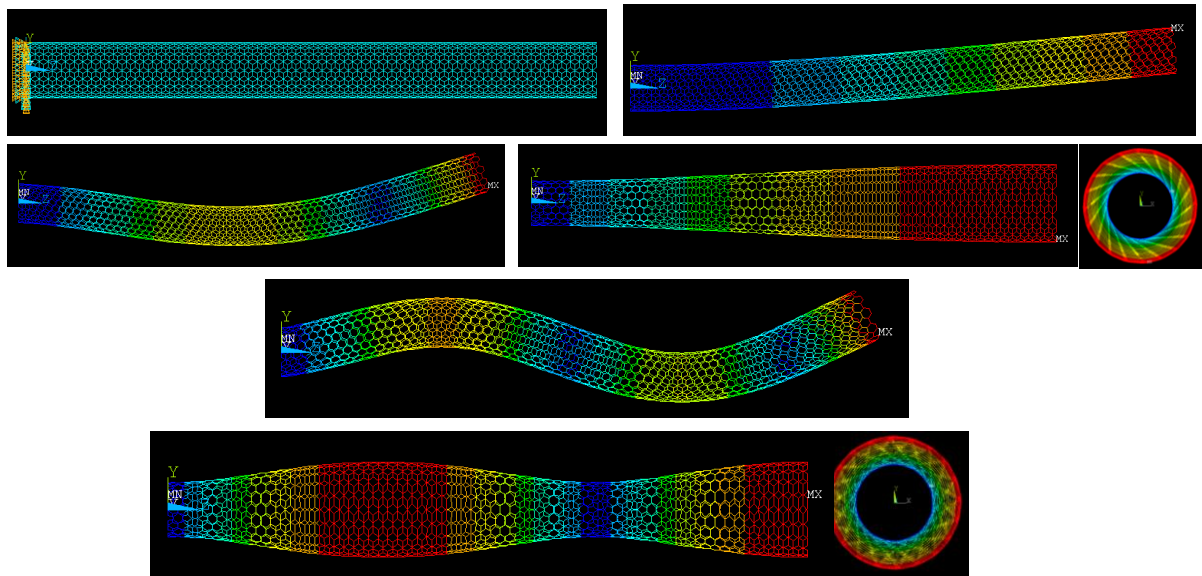


**Fig 26: Different modes of vibration for Cantilevered Armchair configuration with L/D 12 ratio
Bending, Torsion**

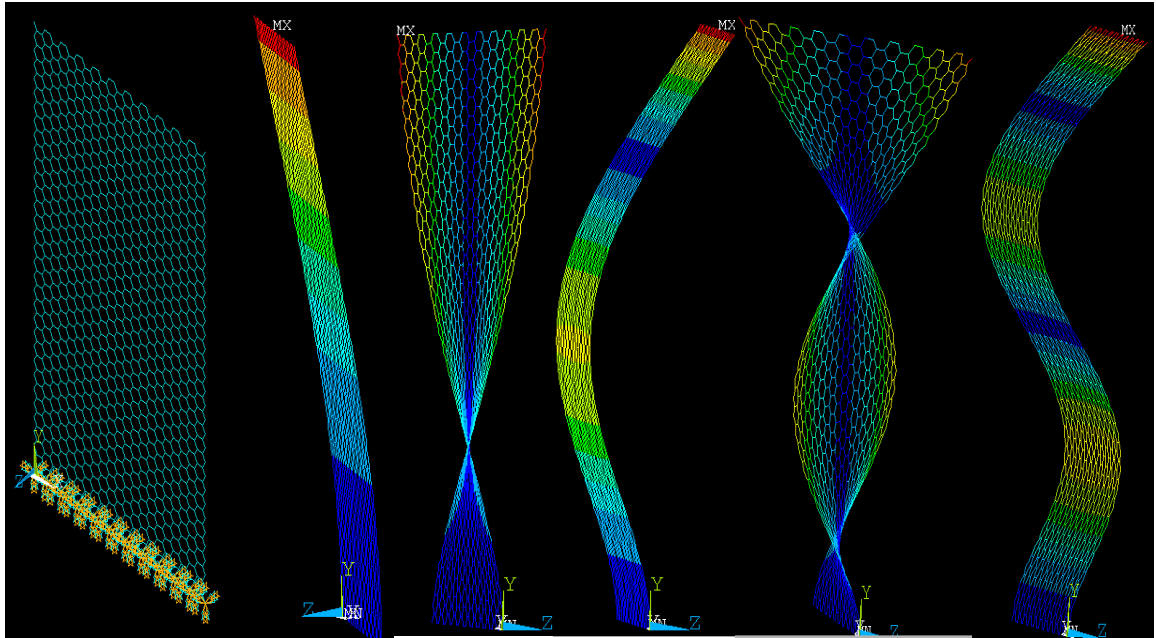


**Fig 27: Different modes of vibration for Cantilevered Graphene with L/D 6 ratio
Bending, Twisting**

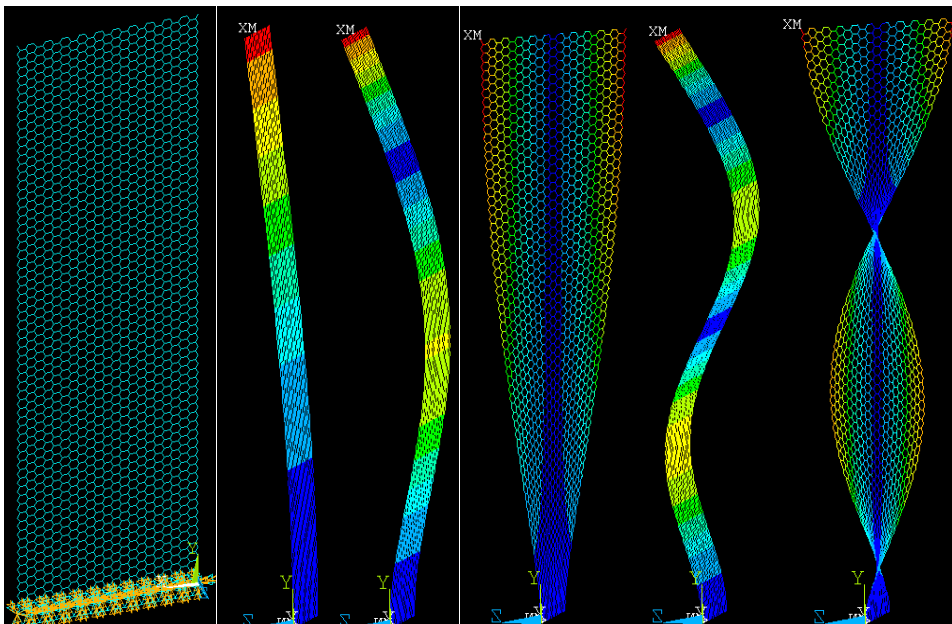


**Fig 28: Different modes of vibration for Cantilevered Graphene with L/D 12 ratio
Bending, Twisting**

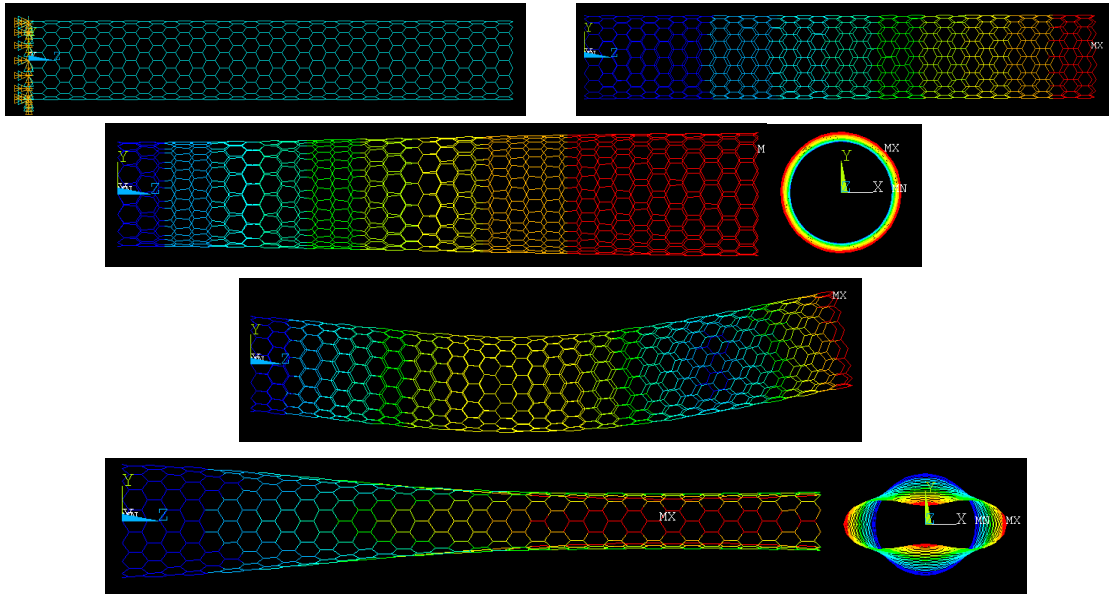


**Fig 29: Different modes of vibration for Cantilevered Zigzag configuration with L/D 6 ratio
Axial, Torsion, Bending, Warping**

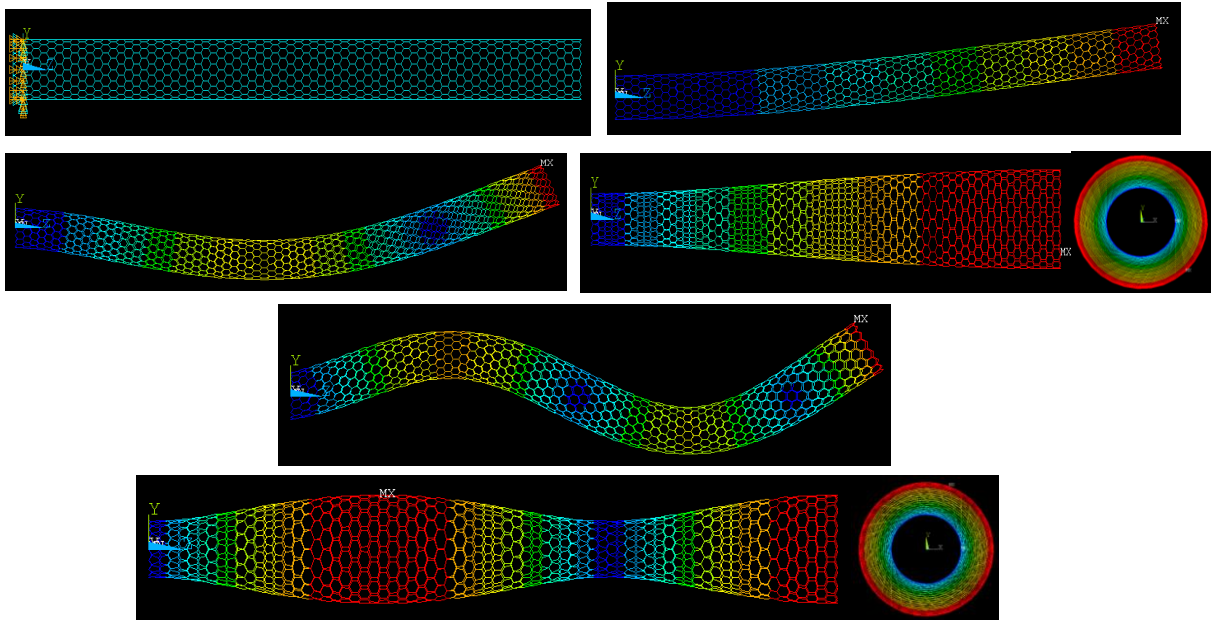


**Fig 30: Different modes of vibration for Cantilevered Zigzag configuration with L/D 12 ratio
Bending, Torsion**

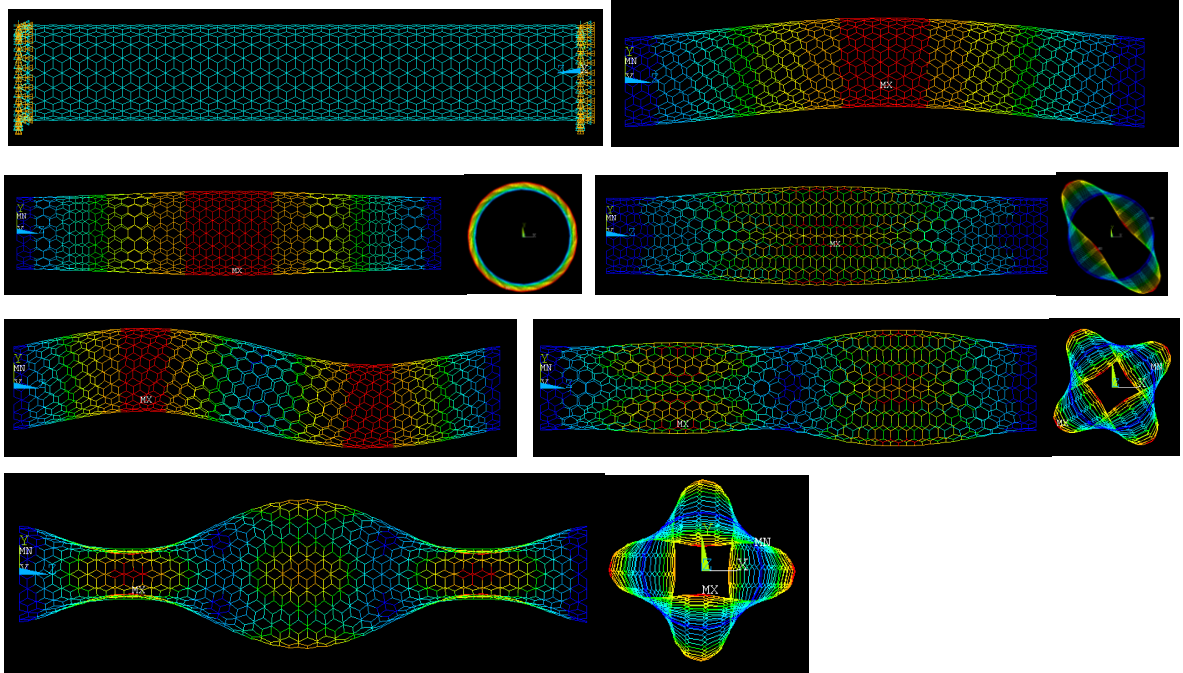


**Fig 31: Different modes of vibration for Fixed Armchair configuration with L/D 6 ratio
Bending, Torsion, Warping**

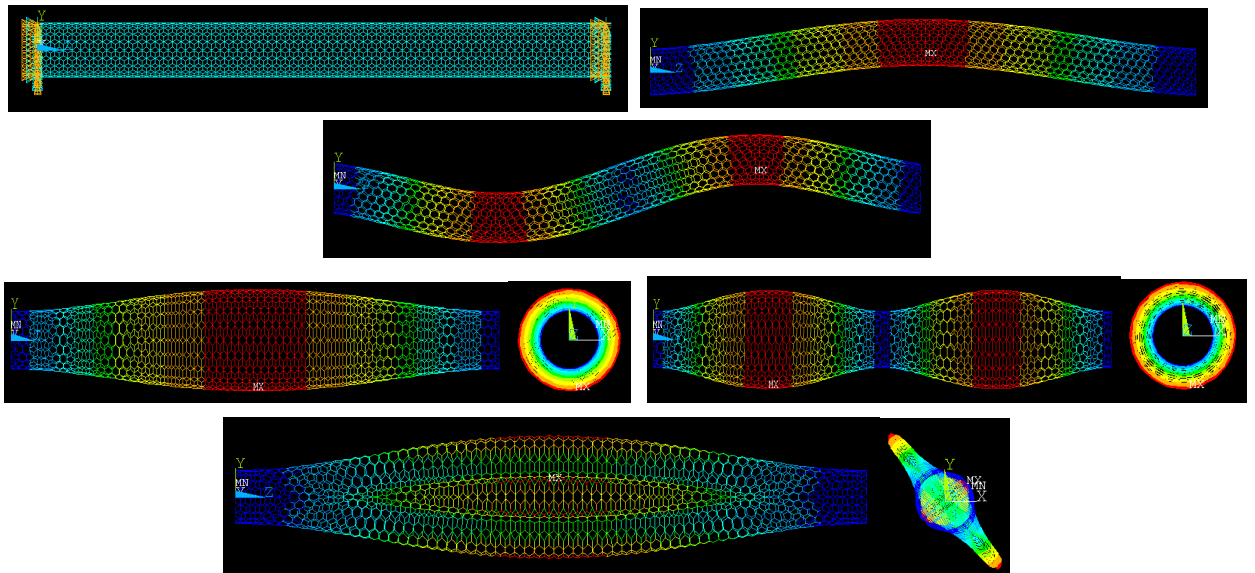


**Fig 32: Different modes of vibration for Cantilevered Armchair configuration with L/D 12 ratio
Bending, Torsion, Warping**

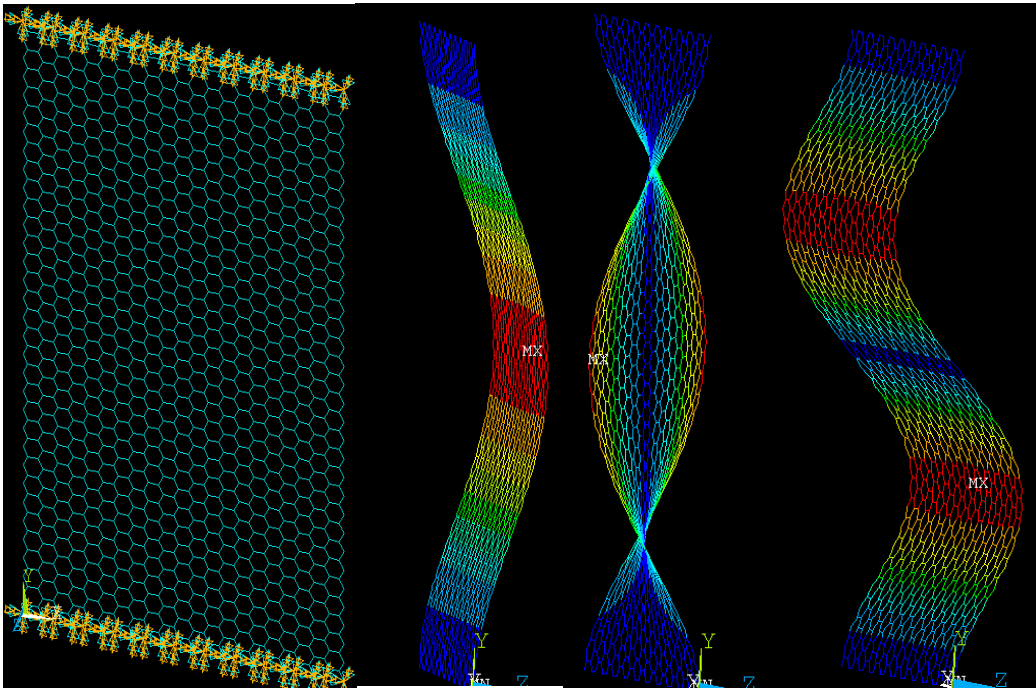


Fig 33: Different modes of vibration for Fixed Graphene with L/D 6 ratio Bending, Twisting

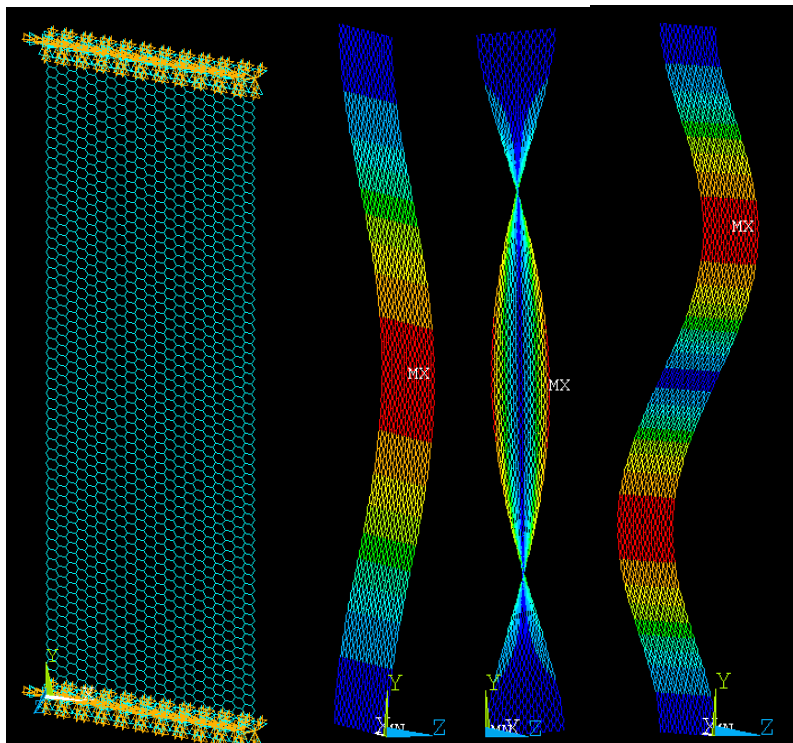
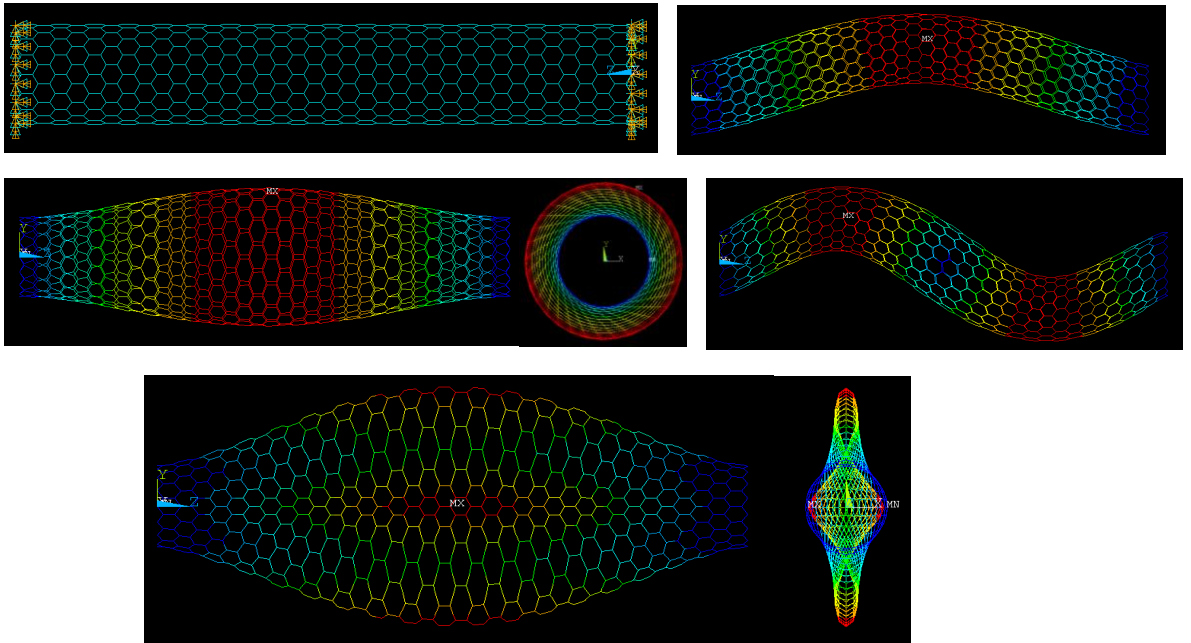
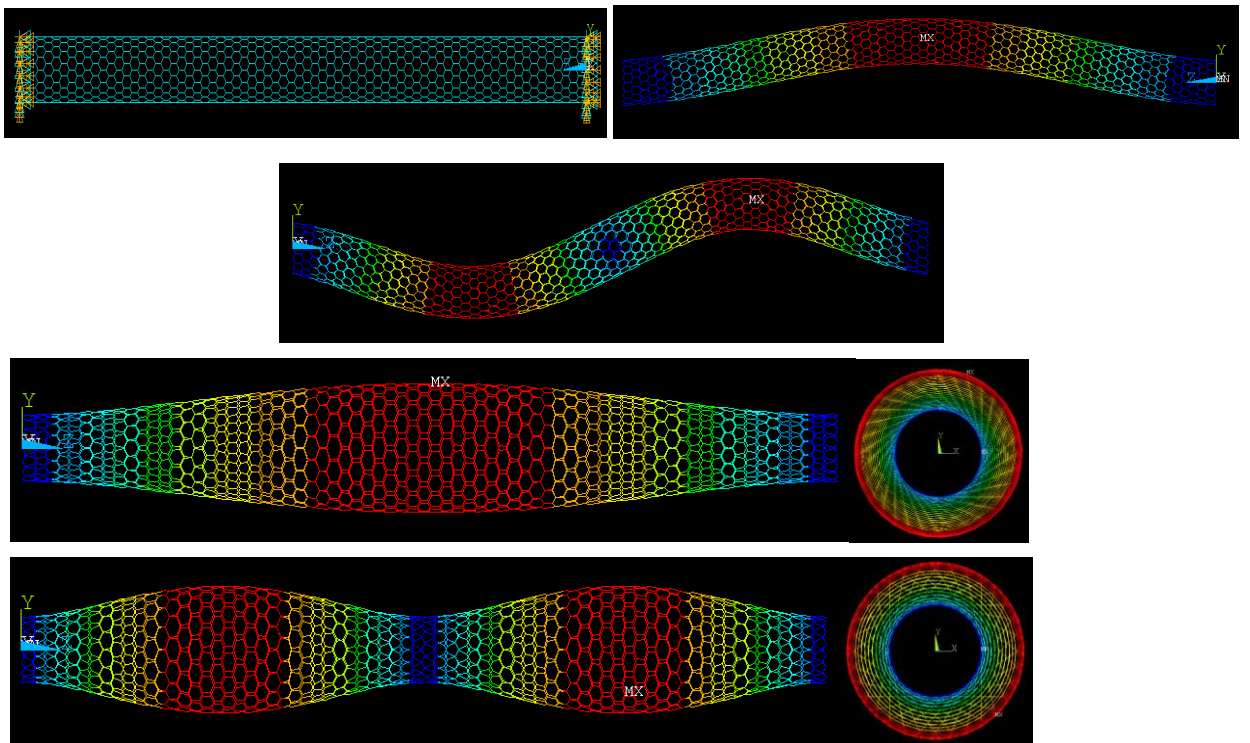


Fig 34: Different modes of vibration for Graphene with L/D 12 ratio Bending, Twisting



**Fig 35: Different modes of vibration for Fixed Zigzag configuration with L/D 6 ratio
Bending, Torsion, Warping**



**Fig 36: Different modes of vibration for Fixed Zigzag configuration with L/D 12 ratio
Bending, Torsion**

Chapter 5

Conclusion

5.1 Conclusion

In this thesis, we have developed a methodology in order to static and dynamic analysis of single walled carbon nanotube under different configurations. The main attraction of this approach is that it is helpful in capturing different modes in less time.

To develop this methodology, we started with the structural details of CNTs and discussed different potential models of the covalent bond systems like C-C bond that exist in carbon nanotube. We found that the Brenner second generation and the Morse modified potential are most accurate potential models of C-C bond. Subsequently, using the Morse modified potential; we used stick-spiral model to estimate elastic modulus of SWCNT based on the available literature. We came up with a compact formula for estimating linear and nonlinear stress-strain relation in SWCNT. In order to increase the applicability of this approach, we used beam element based coupled molecular-structural approach where the equivalent properties of beam element are computed to replace the C-C bond. These properties are then used to do modeling of graphene and carbon nanotube for different configuration and aspect ratios. It is found that this approach can be utilized to effectively capture the dynamics CNTs.

Such method can be extended to do different analysis for multi-walled carbon nanotube. It can be effectively used to improve the design of carbon nanotube based sensors and actuators.

References

- [1] *Carbon Nanotube Science – synthesis, properties and applications*, Peter J.F. Harris, Cambridge University Press, 2009.
- [2] *Carbon Nanotube and Graphene Device Physics*, H.S. Philip Wong and Deji Akinwande, Cambridge University Press, 2011.
- [3] *Carbon Nanotubes – Basic Concepts and Physical Properties*, S. Reich, C. Thomsen and J. Maulztsch, betz-Druck GmbI I, Darmstadt, 2004.
- [4] Guoxin Cao, Xi Chen, and Jeffrey W. Kysar, *Strain Sensing of carbon nanotubes: Numerical analysis of the vibrational frequency of deformed single-wall carbon nanotubes*, Physical Review B 72, 2005, 195412.
- [5] H. Rafil-Tabar, G. A. Mansoori., *Interatomic Potential Models for Nanostructures*. Encyclopedia of Nano Science and Nanotechnology (H. S. Nalwa.), American Scientific Publishers, 2003, pp. 1-17.
- [6] Donald W. Brenner, Olga A Shenderova, Judith A Harrison, Steven J Stuart, Boris Ni and Susan B Sinnott, *second-generation reactive empirical bond order (REBO) potential energy expression for hydrocarbons*, Journal of Physics: Condensed Matter 14, 2002, pp. 783–802.
- [7] Donald W. Brenner, *Empirical Potential for hydrocarbons for use in simulating the chemical vapor deposition of diamond films*, Physical Review B, 1990, Vol. 42, pp. 9458-9471.
- [8] O. Lourie and H.D. Wagner, *Evaluation of Young's modulus of carbon nanotubes by micro-Raman spectroscopy*, Journal of Materials Research, 1998, Vol. 13.
- [9] A. Krishnan, E. Dujardin, T. W. Ebbesen, P. N. Yianilos and M. M. J. Treacy, *Young's modulus of single-walled nanotubes*, Physical Review B, 1998, Vol. 58.
- [10] Tienchong Chang, Jingyan Geng and Xingming Guo, *Prediction of Chirality- and size- dependent elastic properties of single-walled carbon nanotubes via a molecular mechanics model*, The Royal Society A, 462, 2006, pp. 2523-2540.
- [11] J.R. Xiao, B.A. Gama, J.W. Gillespie Jr., *An analytical molecular structural mechanics model for the mechanical properties of carbon nanotubes*, International Journal of Solid Structures 42, 2005, 3075-3092
- [12] H. W. Zhang, J. B. Wang, X. Guo, *Predicting the elastic properties of single-walled carbon nanotubes*, Journal of the mechanics and physics of solids 53, 2005, 1929-1950.
- [13] *The Art of Molecular Dynamics Simulation*, D. C. Rapaport, Cambridge University Press, Cambridge, 2010.

- [14] K.I. Tserpes, P. Papanikos, *Finite element modeling of single-walled carbon nanotubes*, Composites: Part B 36 (2005) 468–477
- [15] Jacob M. Wernik, Shaker A. Meguid, *Atomistic-based continuum modeling of the nonlinear behavior of carbon nanotubes*, Acta Mech 212, 167–179 (2010)
- [16] Ehsan Mohammadpour, Mokhtar Awang, *Nonlinear finite-element modeling of graphene and single-and multi-walled carbon nanotubes under axial tension*, Appl Phys A (2012) 106:581–588
- [17] Usik Lee, Hyukjin Oh and Sungjun You (2007), *Natural Frequencies of Single-Walled Carbon Nanotubes*, Proceedings of the 2nd IEEE International, Conference on Nano/Micro Engineered and Molecular Systems, January 16-19, 2007, Bangkok, Thailand, 13-16.
- [18] Lee, J. H., & Lee, B. S. (2012). Modal analysis of carbon nanotubes and nanocones using FEM. *Computational Materials Science*, 51(1), 30-42. Elsevier B.V. doi:10.1016/j.commat.2011.06.041